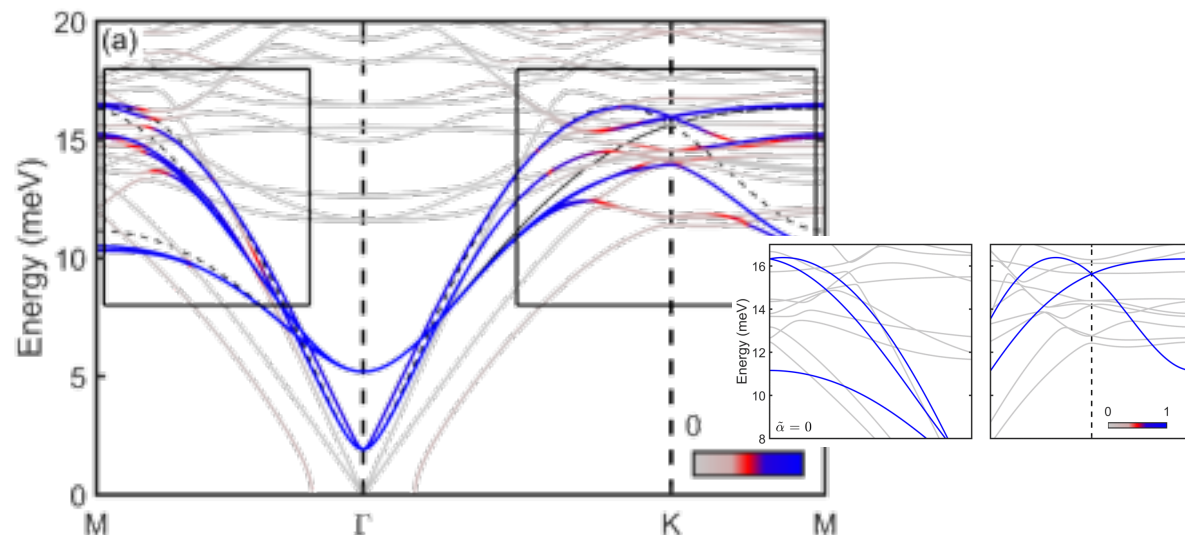
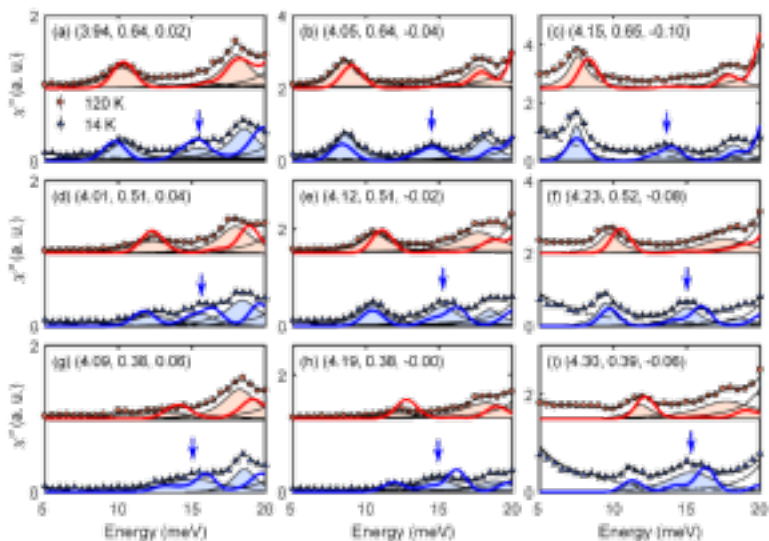


# Magnon-magnon/phonon coupling in two-dimensional triangular lattice antiferromagnets



Je-Geun Park

Center for Correlated Electron Systems, Institute for Basic Science

Dept. Physics & Astronomy

Seoul National University

- ◆ Why magnon-magnon/phonon coupling in 2D TAF?
- ◆ A Tale of Two Cities: magnon-magnon/phonon couplings in  $\text{YMnO}_3$ 
  - Magnons measured by inelastic neutron scattering
  - Phonons measured by inelastic X-ray scattering

- ◆ Outlook

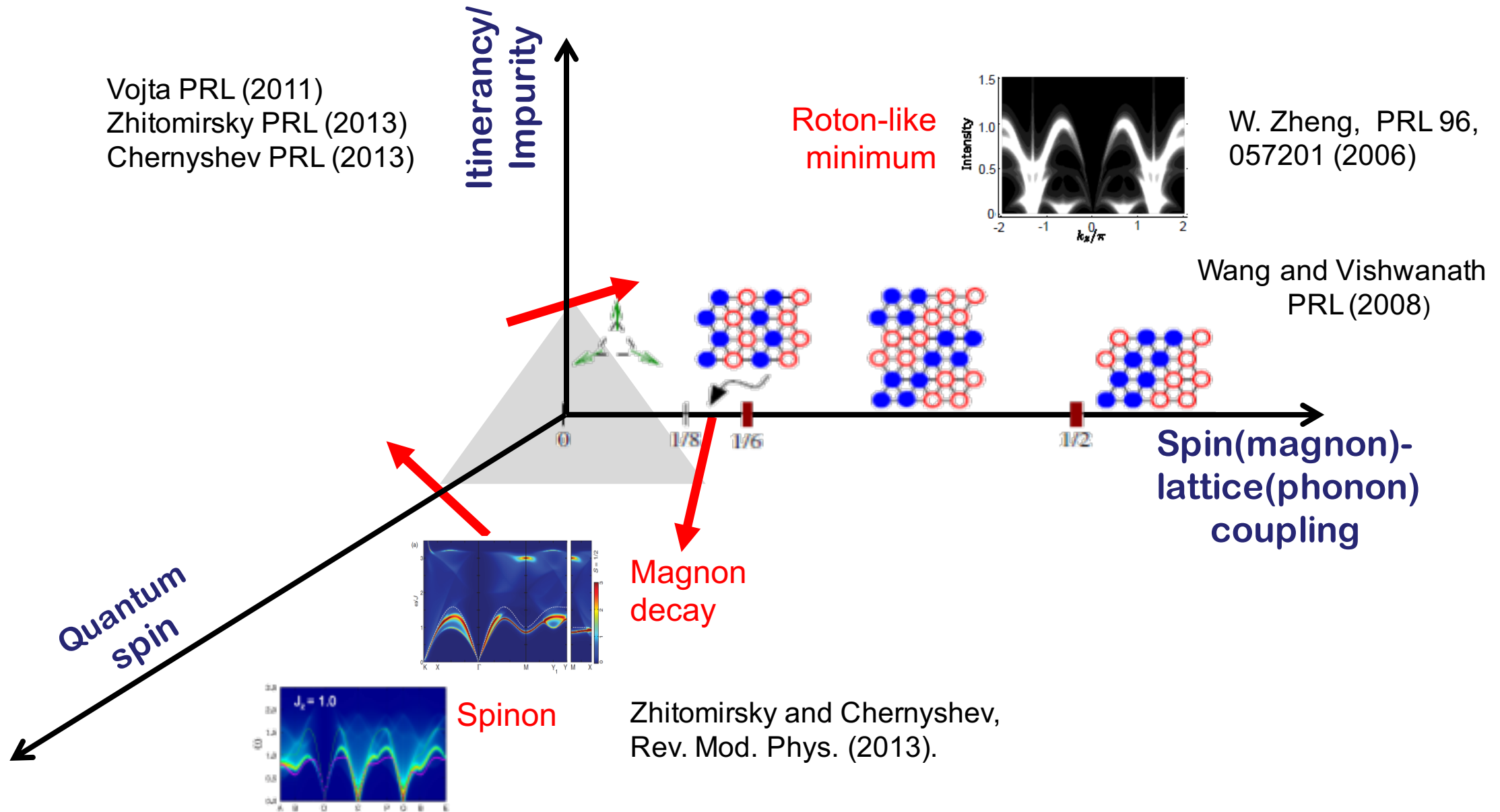


### Posters

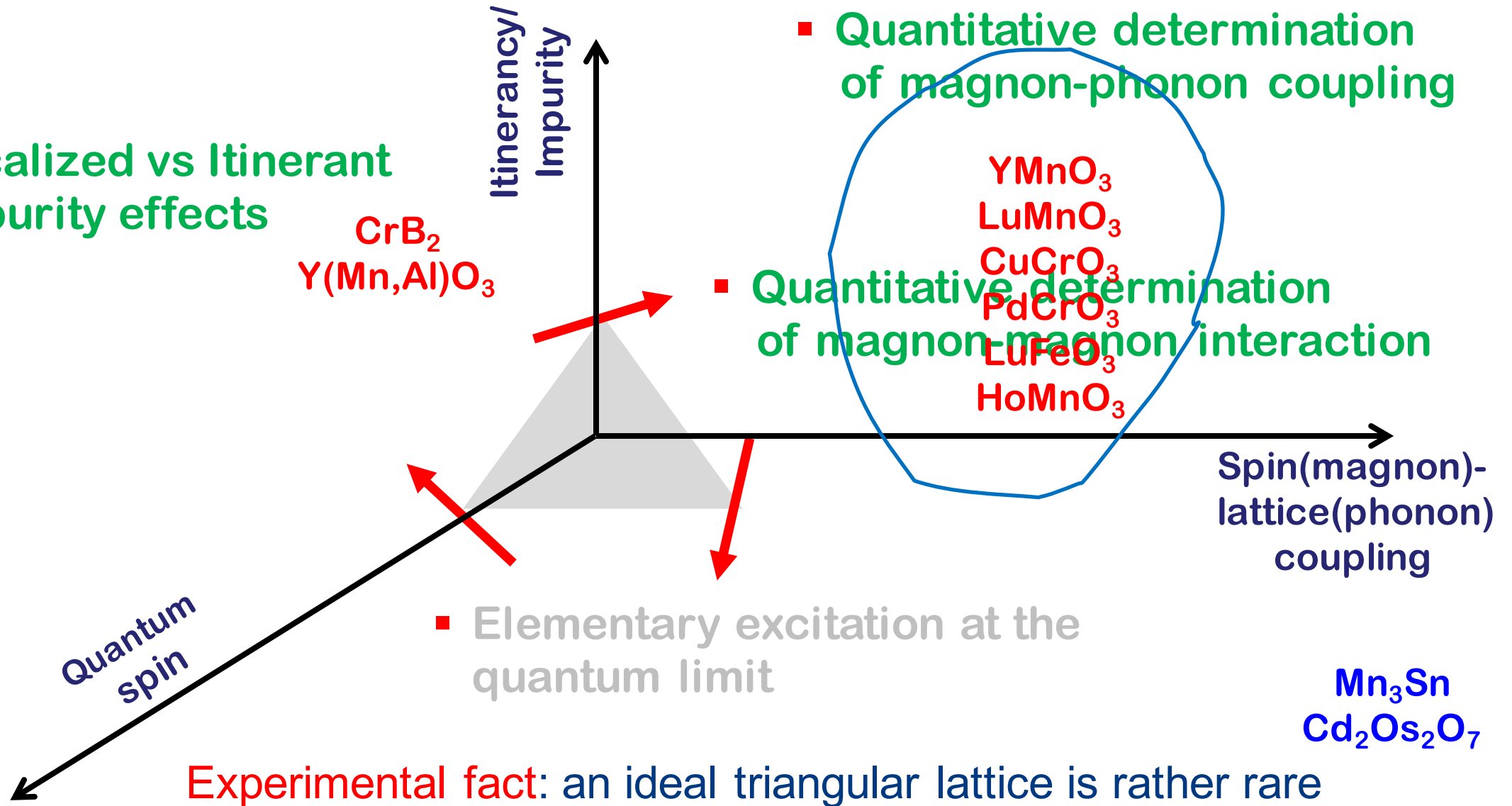
- Spin texture and its dynamics of Al-doped triangular lattice antiferromagnet  $\text{h-YMnO}_3$ , Kiso Park
- Magnetic excitations in non-collinear metallic antiferromagnet  $\text{CrB}_2$ , Pyeongjae Park



# Triangular Antiferromagnets



- Localized vs Itinerant
- Impurity effects



- Quantitative determination of magnon-phonon coupling

- Quantitative determination of magnon-magnon interaction

- Elementary excitation at the quantum limit

Experimental fact: an ideal triangular lattice is rather rare among magnetic systems.

## Interaction of Spin Waves and Ultrasonic Waves in Ferromagnetic Crystals\*

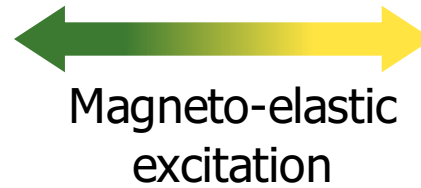
C. KITTEL

Department of Physics, University of California, Berkeley, California

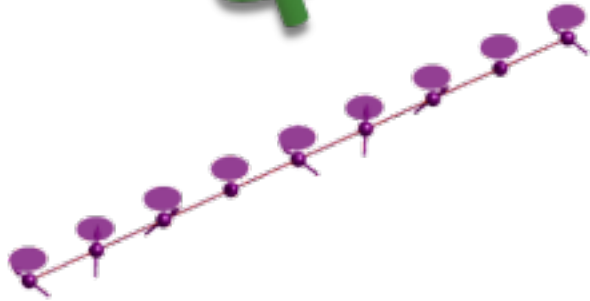
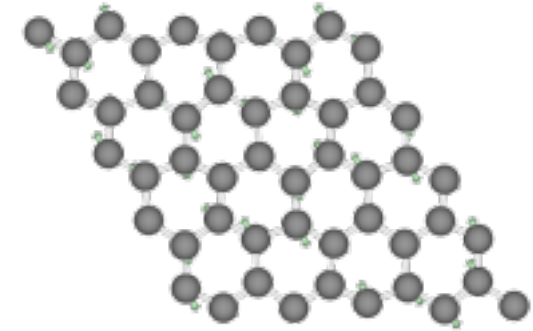
(Received January 9, 1958)



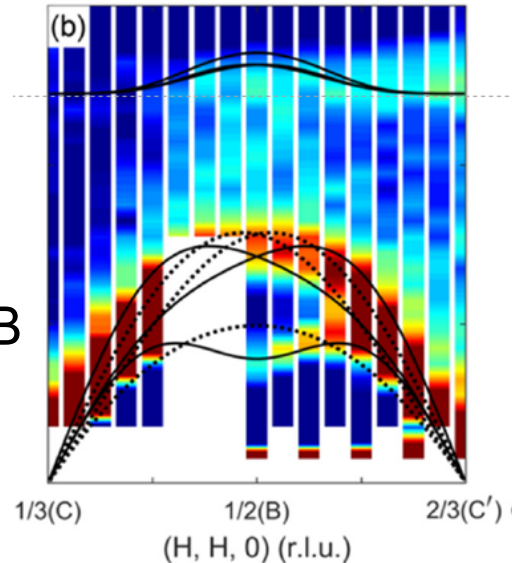
Magnon (spin waves)



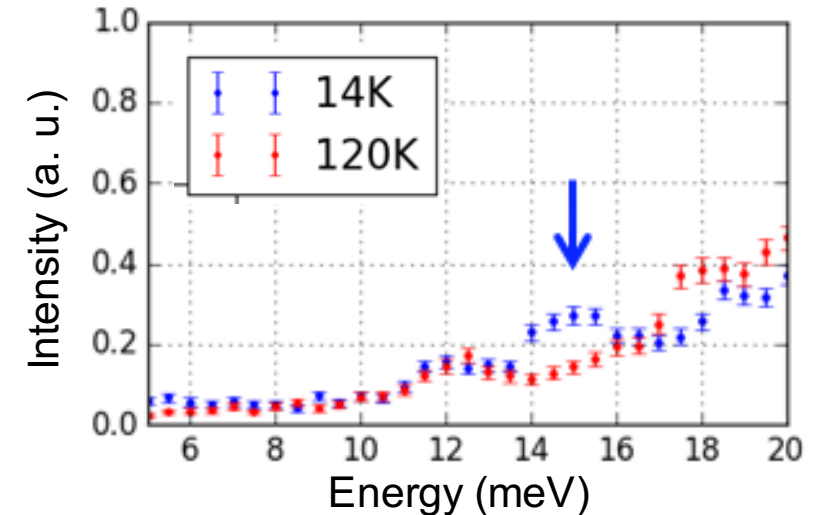
Phonon



Inelastic Neutron Scattering



Inelastic X-ray Scattering



- ✓ Fundamental issue for magnetism
- ✓ Spintronics applications
- ✓ Thermoelectric materials
- ✓ Topological Physics: K. H. Lee et al., PRB (2018, 2019); H. R. Kim et al., to be published

Diagonal components

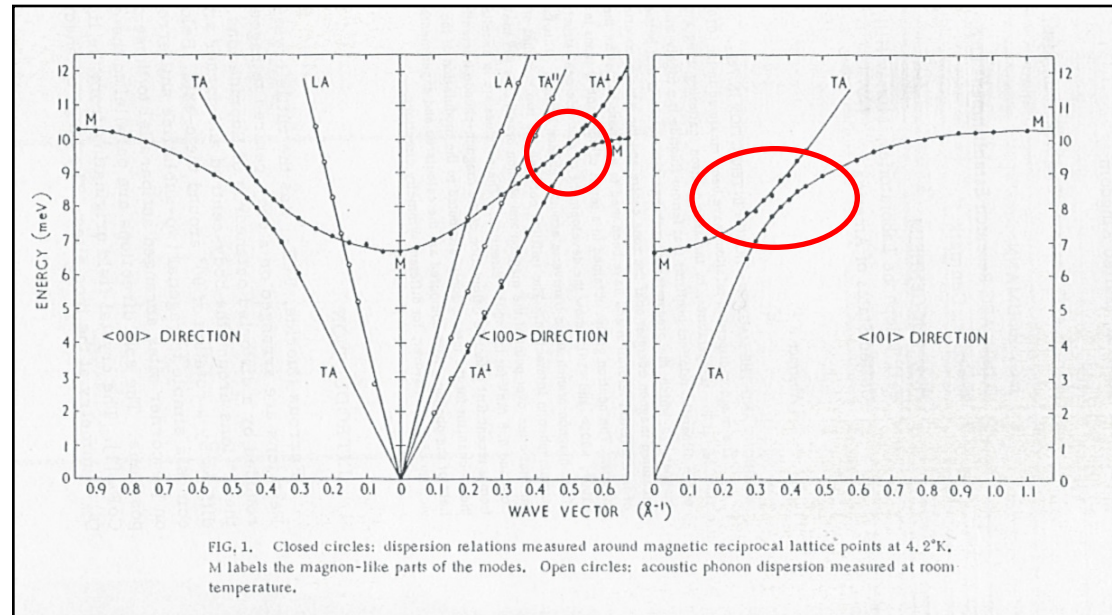
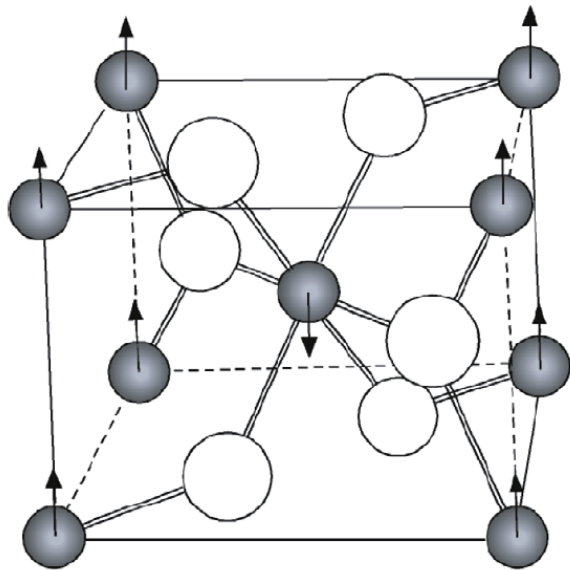
$$H_{mp} = \underbrace{U}_{\substack{\text{1 phonon} \\ \downarrow}} \left( \delta J \sum_{i,j,\alpha=x,y,z} \mathbf{S}_i \cdot \mathbf{S}_j + \delta D \sum_i (S_i^z)^2 + \delta K_1 \sum_{i,j,\alpha \neq \beta} S_i^\alpha S_j^\beta + \delta K_2 \sum_{i,\alpha \neq \beta} S_i^\alpha S_i^\beta \right)$$

Terms quadratic in  $S_i^x, S_i^y$

Off-diagonal components

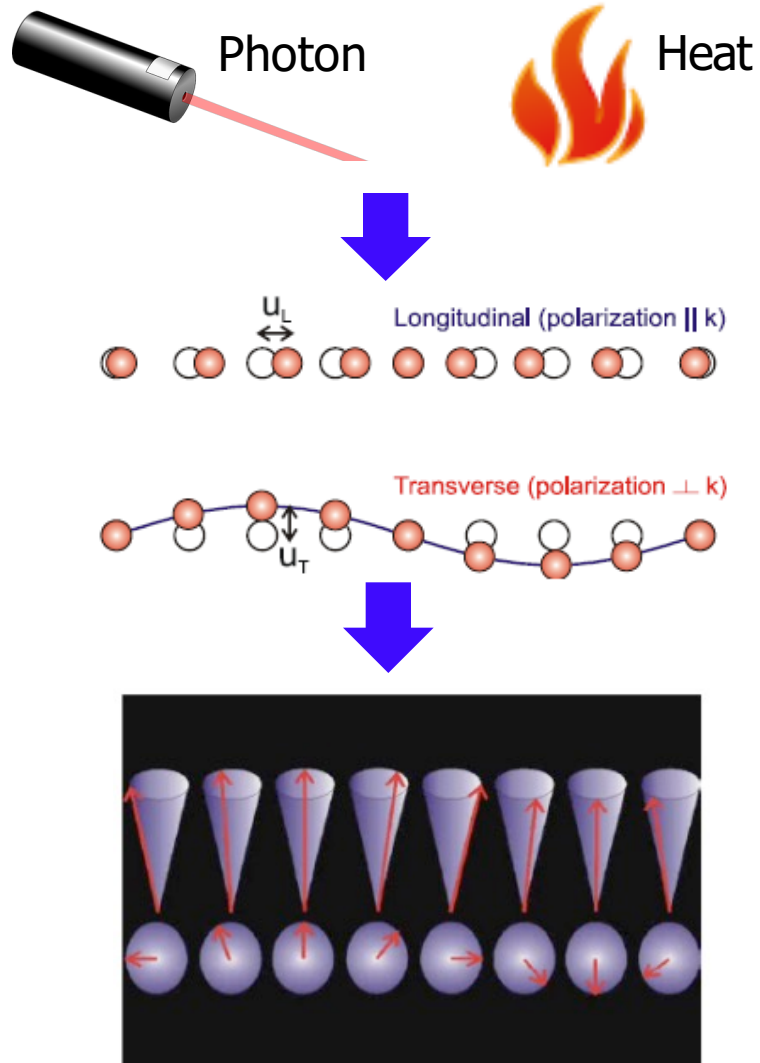
Terms linear in  $S_i^x, S_i^y$ : 1 magnon

FeF<sub>2</sub>



## Spintronics: spins as data storage

Writing process by photon & heat



nature  
materials

LETTERS

PUBLISHED ONLINE: 21 AUGUST 2011 | DOI: 10.1038/NMAT3099

## Long-range spin Seebeck effect and acoustic spin pumping

K. Uchida<sup>1,2</sup>, H. Adachi<sup>2,3</sup>, T. An<sup>1,2</sup>, T. Ota<sup>1,2</sup>, M. Toda<sup>4</sup>, B. Hillebrands<sup>5</sup>, S. Maekawa<sup>2,3</sup>  
and E. Saitoh<sup>1,2,3,6</sup>★

## Photodrive of magnetic bubbles via magnetoelastic waves

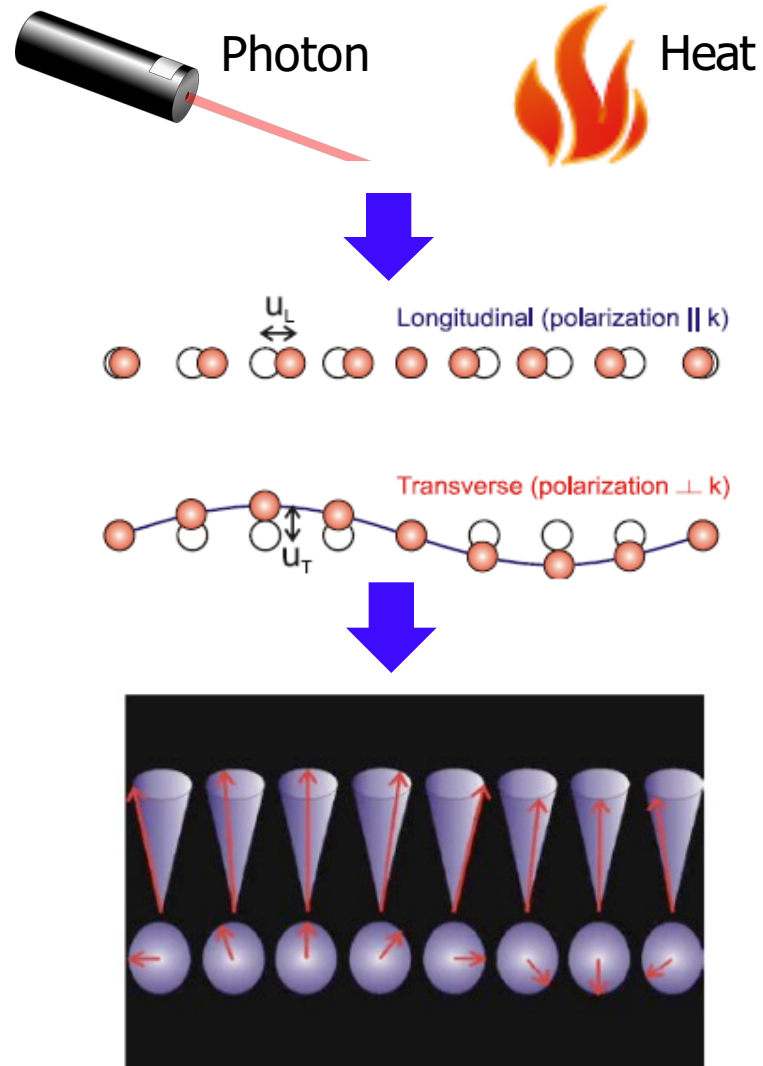
Naoki Ogawa<sup>a,1</sup>, Wataru Koshibae<sup>a</sup>, Aron Jonathan Beekman<sup>a</sup>, Naoto Nagaosa<sup>a,b</sup>, Masashi Kubota<sup>a,c,2</sup>,  
Masashi Kawasaki<sup>a,b</sup>, and Yoshinori Tokura<sup>a,b</sup>

<sup>a</sup>RIKEN Center for Emergent Matter Science, Wako, Saitama 351-0198, Japan; <sup>b</sup>Department of Applied Physics and Quantum Phase Electronics Center, University of Tokyo, Tokyo 113-8656, Japan; and <sup>c</sup>Research and Development Headquarters, ROHM Company, Ltd., Kyoto 615-8585, Japan

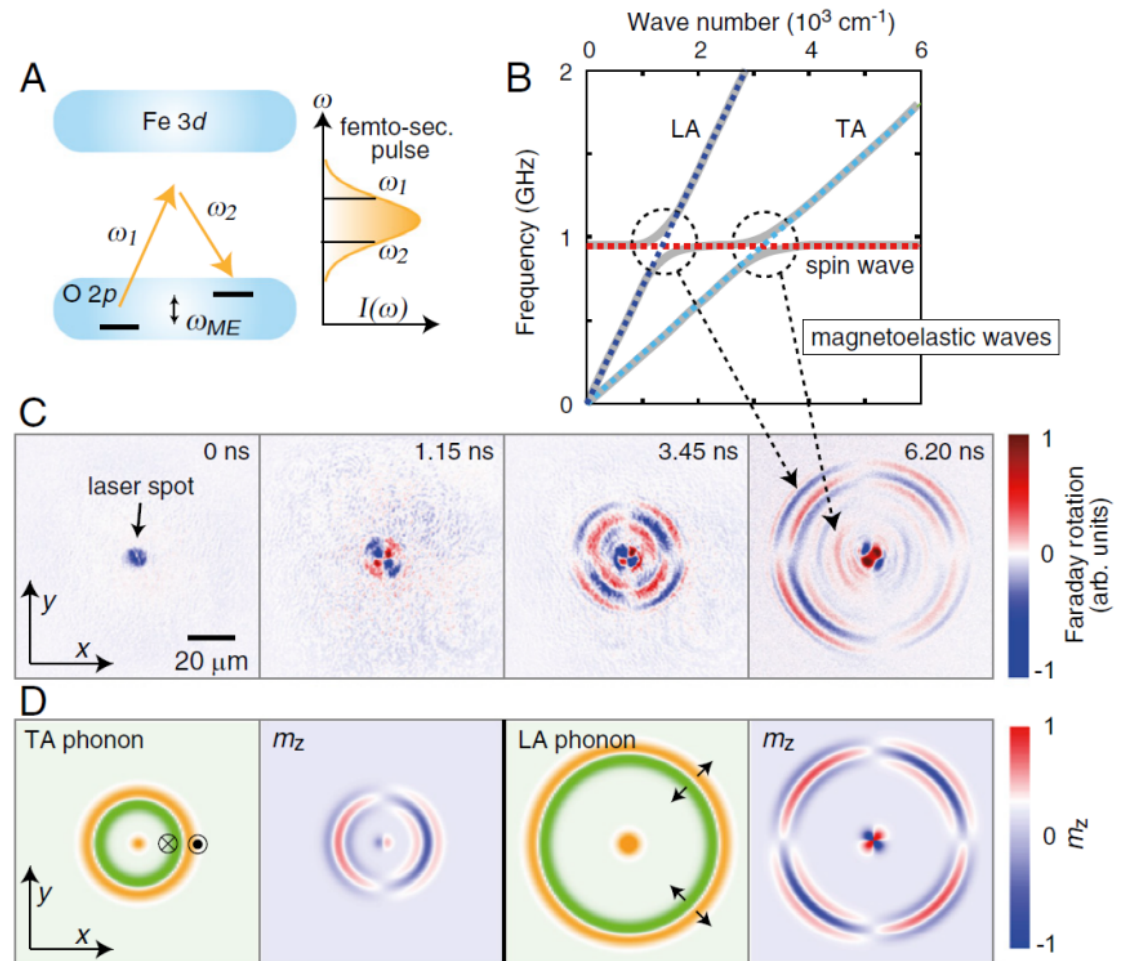
Edited by Chia-Ling Chien, The Johns Hopkins University, Baltimore, MD, and accepted by the Editorial Board June 6, 2015 (received for review February 27, 2015)

- Magnon-phonon coupling is important for spin conversion.
- Conversion factor  $\propto$  coupling strength

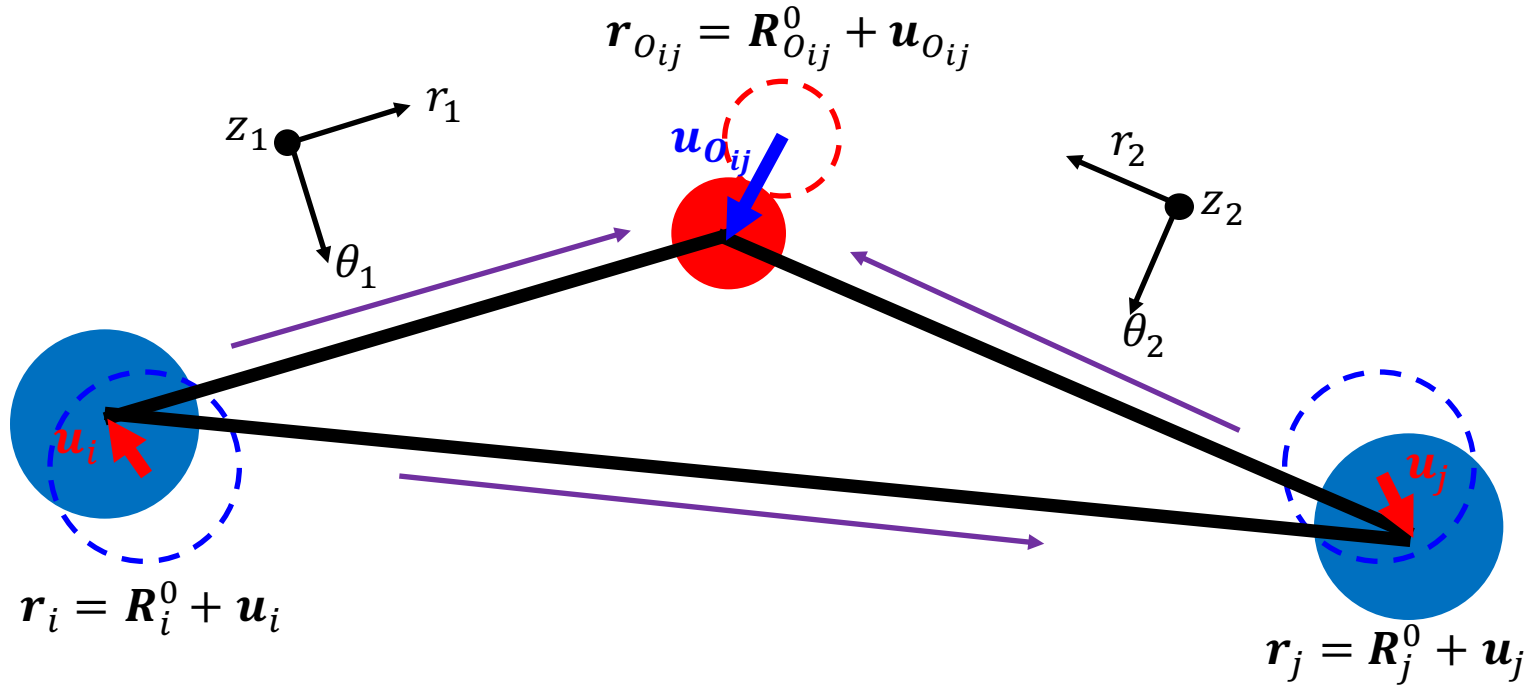
**Spintronics: spins as data storage**  
 Writing process by photons & heat



## Photo-induced magnetic domain in YIG





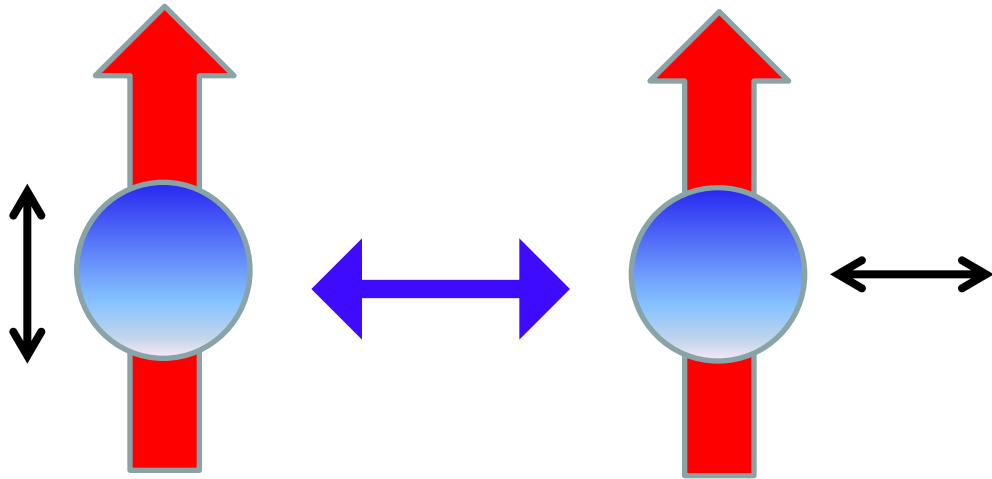


$$H = H_{Heis} + H_{lattice} = \sum_{ij} J_{ij} \mathbf{S}_i \cdot \mathbf{S}_j + H_{lattice}$$

$$J_{ij}(\mathbf{R}_i, \mathbf{R}_j, \mathbf{R}_{Oij}) = J_0 + (\mathbf{u}_1 \cdot \nabla_1 + \mathbf{u}_2 \cdot \nabla_2 + \mathbf{u}_3 \cdot \nabla_3) J_{ij} + \dots$$

$$(\mathbf{u}_1 \cdot \nabla_1 + \mathbf{u}_2 \cdot \nabla_2 + \mathbf{u}_3 \cdot \nabla_3) J_{ij} = \underbrace{(\mathbf{u}_{Oij} - \mathbf{u}_i) \cdot \nabla_1}_{\text{Superexchange-striction}} J_{ij} + \underbrace{(\mathbf{u}_{Oij} - \mathbf{u}_j) \cdot \nabla_2}_{\text{Direct exchange-striction}} J_{ij} + \underbrace{(\mathbf{u}_j - \mathbf{u}_i) \cdot \nabla_3}_{\text{Direct exchange-striction}} J_{ij}$$

- Exchange energy is dominant in most 3d TM based magnets
- No linear coupling in collinear spin structure



Longitudinal  
spin fluctuation

$$S_i^z = S - b_i^\dagger b_i$$

Transverse  
spin fluctuation

$$S_i^x, S_i^y = b_i^\dagger, b_i$$

$$H = J \sum_{i,j} \mathbf{S}_i \cdot \mathbf{S}_j$$

$$= J \sum_{i,j} (S_i^x S_j^x + S_i^y S_j^y + S_i^z S_j^z)$$

$$H_{mp} = \underbrace{U}_{\text{1 phonon}} \delta J S \sum_{i,j} \underbrace{(S_i^x S_j^x + S_i^y S_j^y + S_i^z S_j^z)}_{\text{2 magnon}}$$

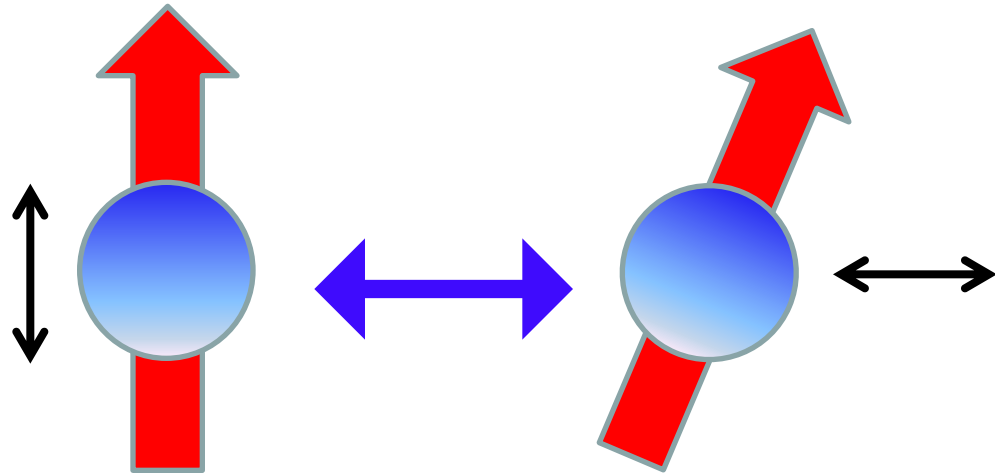
1 phonon

2 magnon

- Noncollinear magnetic structure: Transverse-longitudinal coupling  
→ Direct mixing of magnons and phonons



Joosung Oh  
PhD Thesis  
(2017)



Longitudinal  
spin fluctuation  
 $S_i^z = S - b_i^\dagger b_i$

Transverse  
spin fluctuation  
 $S_i^x, S_i^y = b_i^\dagger, b_i$

$$H = J \sum_{i,j} \mathbf{S}_i \cdot \mathbf{S}_j$$

$$= JS \sum_{i,j} (S_i^x + S_i^y + \dots)$$

$$H_{mp} = \underbrace{U}_{1 \text{ phonon}} \delta JS \sum_{i,j} \underbrace{(S_i^x + S_i^y + \dots)}_{1 \text{ magnon}}$$

- Lattice & spin modulation → phonon & magnon operators
- Numerical diagonalization of Hamiltonian
- Calculation of dynamical spin structure factor

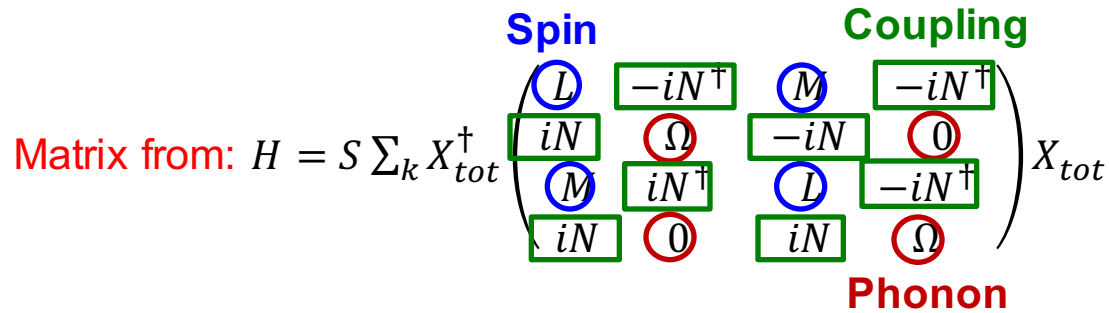
Joosung Oh  
 PhD Thesis  
 (2017)



$$H = H_{spin} + \hbar \sum_{i=1}^{90} \omega_i b_k^\dagger b_k + \frac{\alpha J}{2d} \sum_{ij} (e_{o_{ij}i} \cdot \mathbf{U}_i + e_{o_{ij}j} \cdot \mathbf{U}_j) \mathbf{S}_i \cdot \mathbf{S}_j$$

**Lattice modulation:**  $\mathbf{U}_{j,l} = \sqrt{\frac{\hbar}{2Nm_j \omega_{k\lambda}}} \sum_{k,\lambda} \mathbf{V}_{j,k\lambda} e^{ik \cdot (R_l + r_j)} (b_{k\lambda} + b_{-k\lambda}^\dagger)$

**Spin modulation:**  $\mathbf{S}_i^- \approx \sqrt{2S} a_i^\dagger$



$$X_{tot} = \left( \underbrace{a_{k_1} \dots a_{k_6}}_{\text{magnon}} \underbrace{b_{k_1} \dots b_{k_\lambda}}_{\text{phonon}} \dots a_{-k_1}^\dagger \dots a_{-k_6}^\dagger b_{-k_1}^\dagger \dots b_{-k_\lambda}^\dagger \dots \right)^T$$

Estimated  $\alpha$  For YMnO<sub>3</sub>

$$\alpha = \frac{d(P_0)}{T_N(P_0)} \frac{\partial T_N / \partial P}{(\partial d / \partial P)} = 14$$

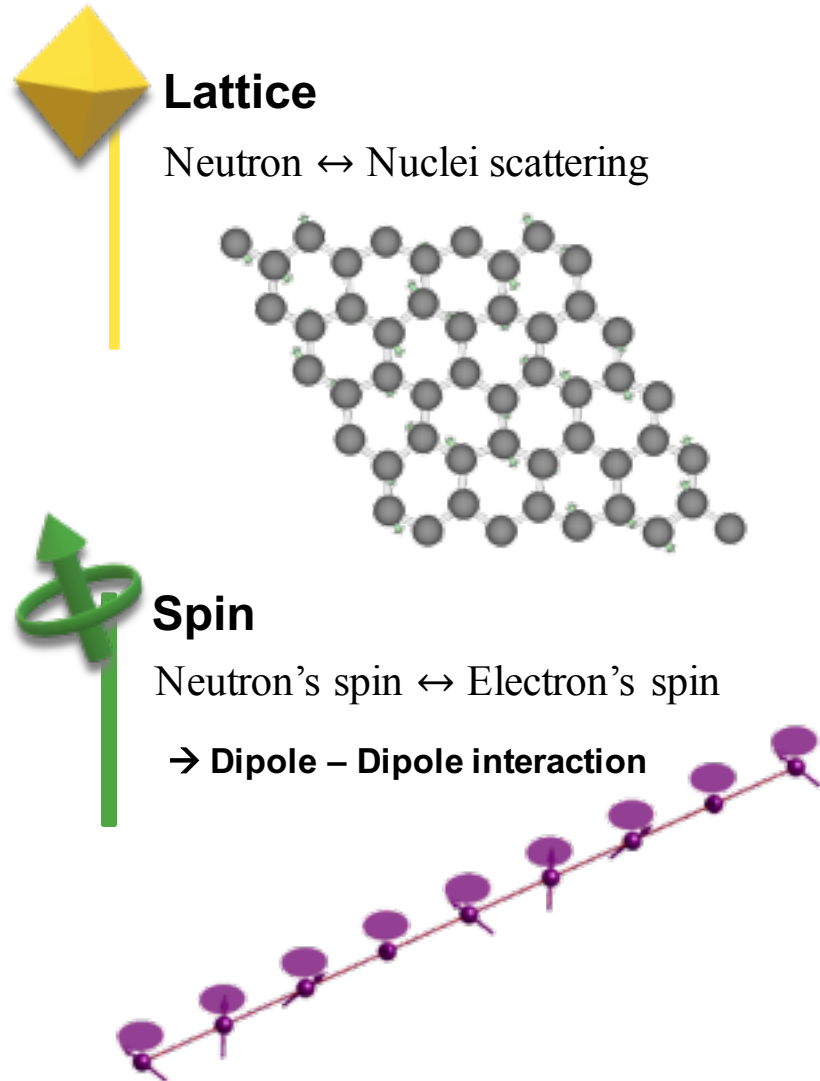
- T. Lancaster et al., PRL 98, 197203 (2007)
- D. P. Kozlenko, JGP et al., JETP 82, 193 (2005)

La<sub>2</sub>CuO<sub>4</sub>:  $\alpha = 6 \sim 7$

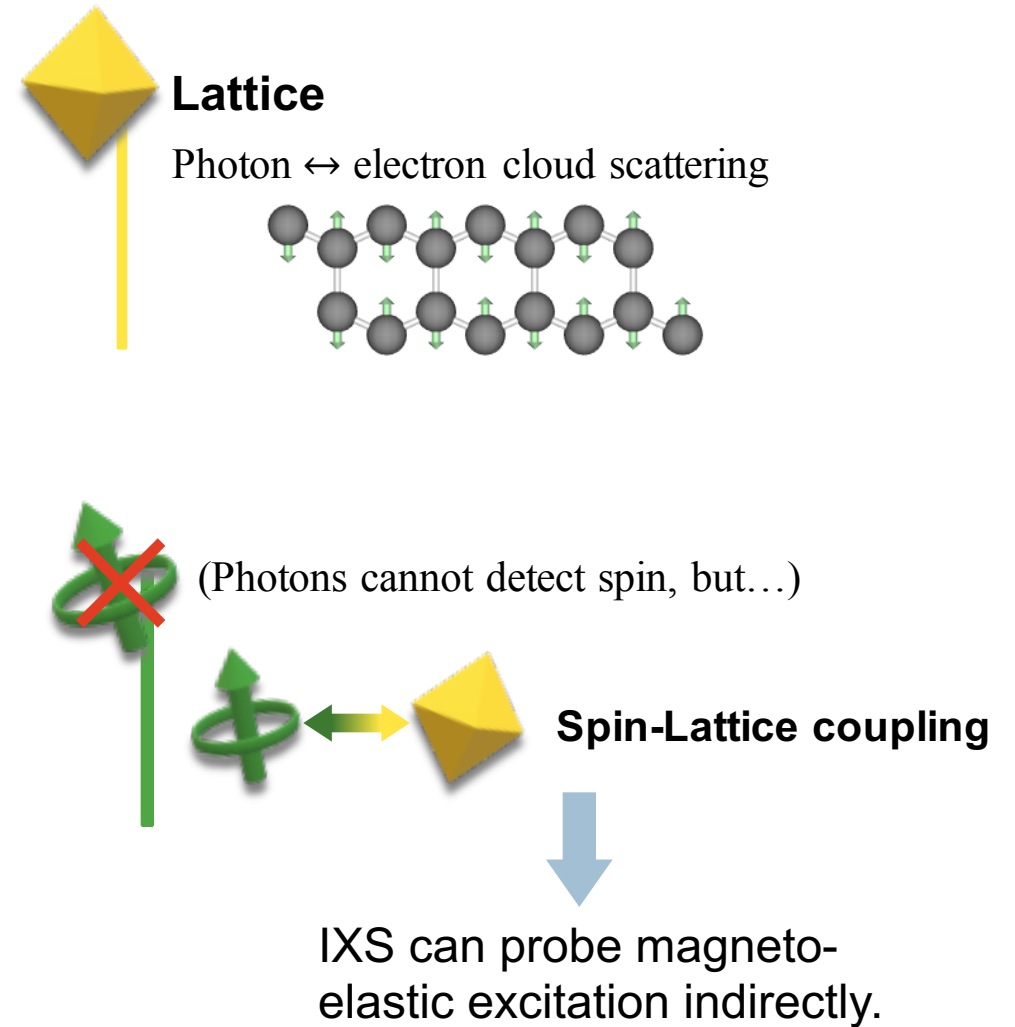
CuCrO<sub>2</sub>:  $\alpha = 30$

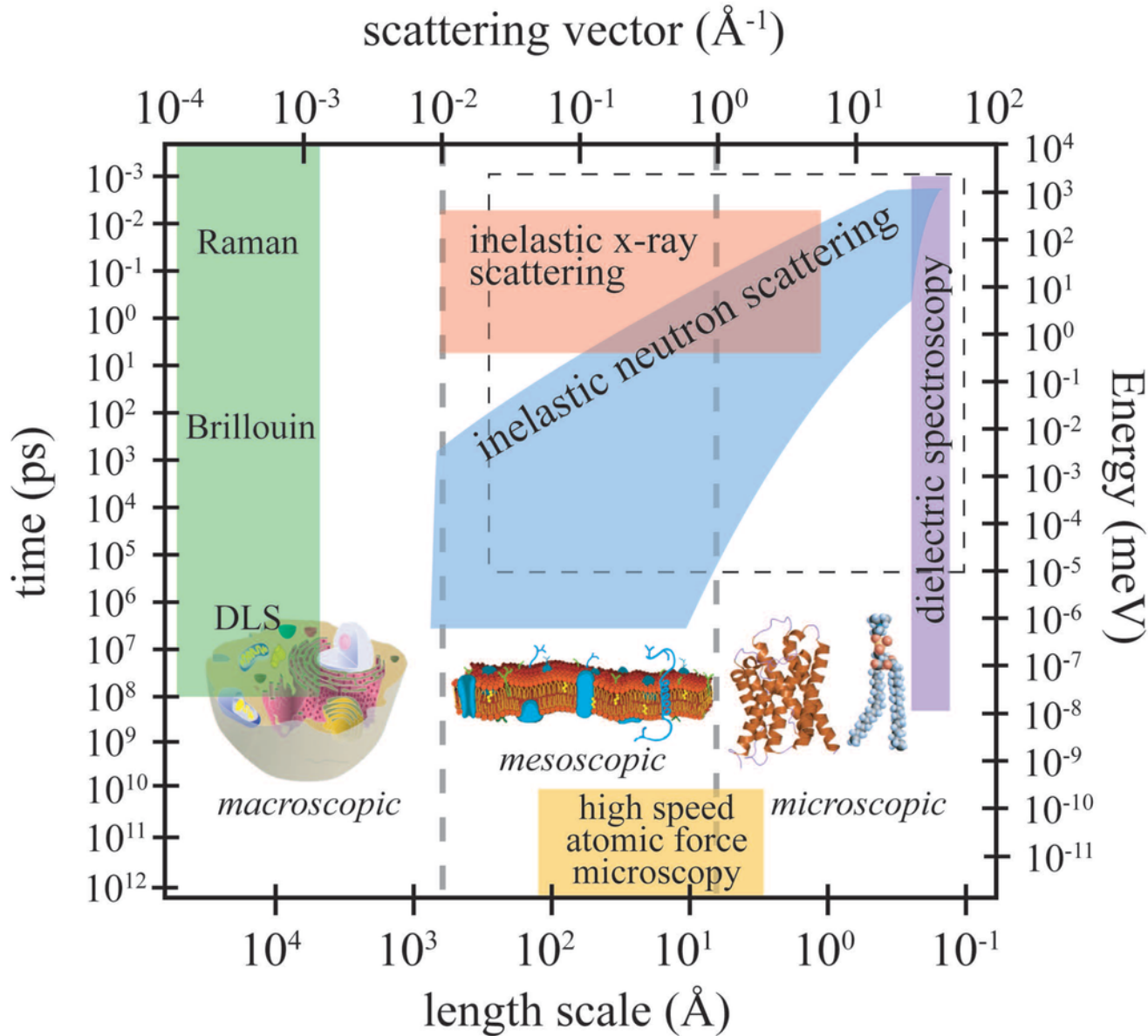
- M. C. Aronson et al., PRB 44, 4657 (1991)
- K. Park, JGP et al., PRB 94, 104421 (2016)

## Inelastic Neutron Scattering



## Inelastic X-ray Scattering





- **Wavelengths** of neutrons and x-ray are similar to atomic spacing!
- **Energy** of neutrons and x-ray are similar to elementary excitations in solids!

### Advantage of Inelastic neutron scattering

- Probes both spin & lattice excitation
- Good energy resolution
- Sensitive to light atoms

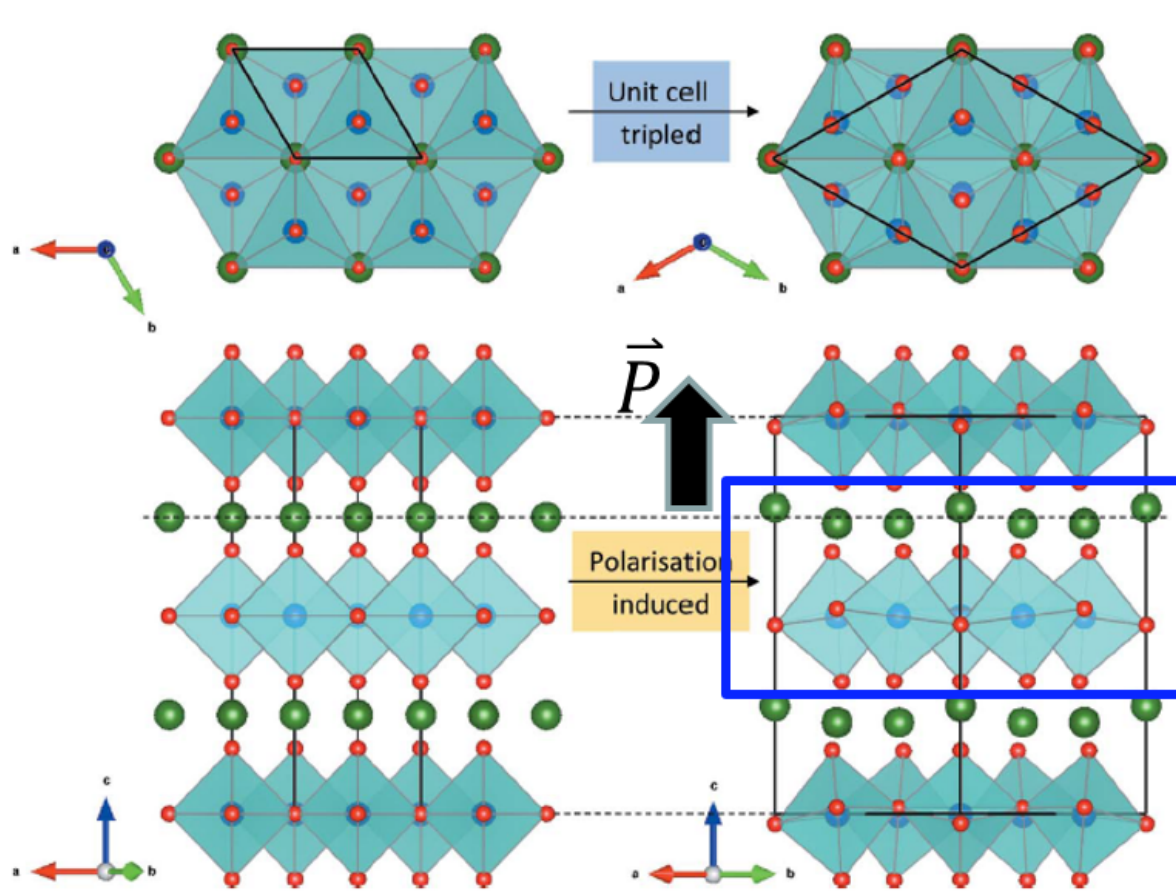
### Advantage of Inelastic x-ray scattering

- Probes lattice vibration
- Good momentum resolution
- Low background
- Small sample down to  $10\mu\text{m}$  and  $100\text{nm}$  film

# Magnon-Magnon/Phonon Coupling in hexagonal Manganites

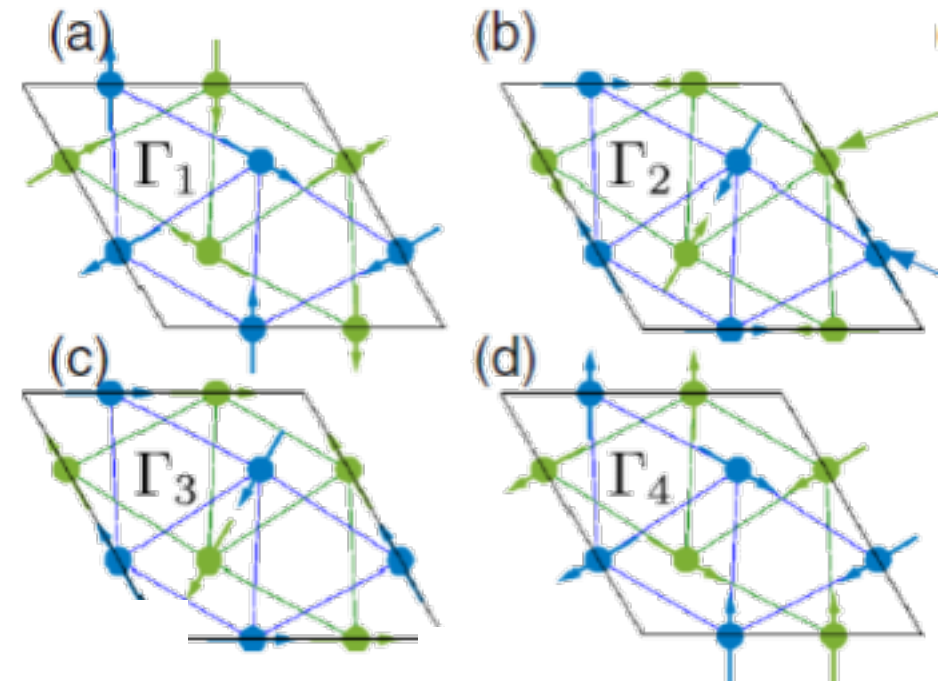
Inelastic Neutron and X-ray Scattering

- Structural transition from paraelectric (P6<sub>3</sub>/mmc) to ferroelectric (P6<sub>3</sub>cm) below T<sub>c</sub>~1250 K
- Mn atoms form triangular layers
- 120° noncollinear magnetic order below T<sub>N</sub> due to geometrical frustration

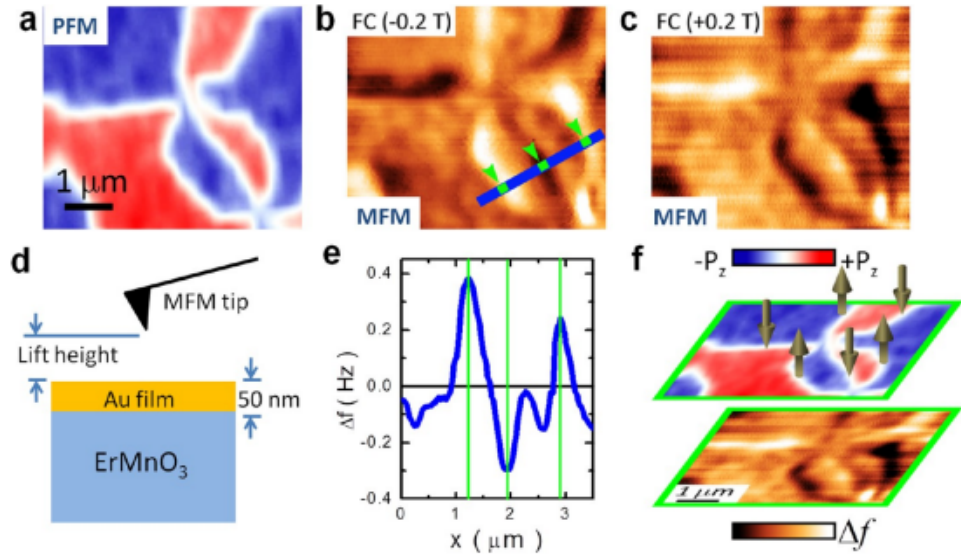


- YMnO<sub>3</sub>: T<sub>N</sub>=75 K,  $\theta_{CW}$ =705 K
- LuMnO<sub>3</sub>: T<sub>N</sub>=90 K,  $\theta_{CW}$ =887 K

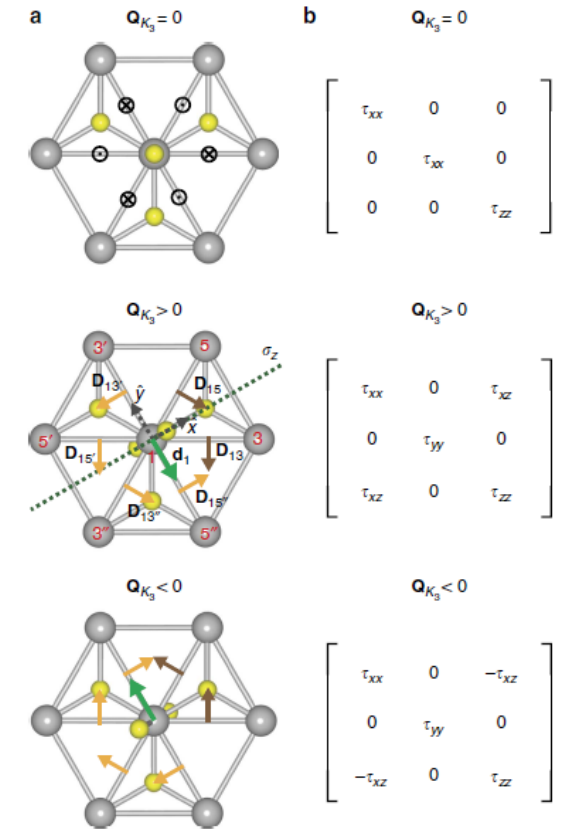
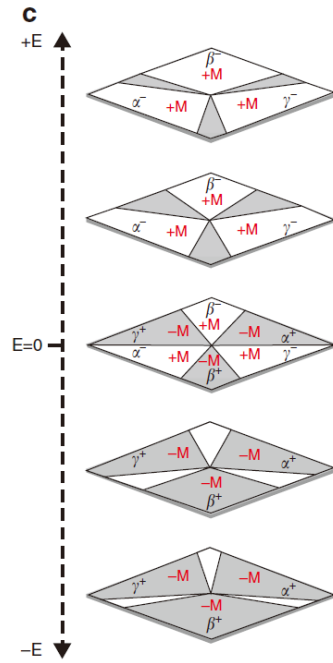
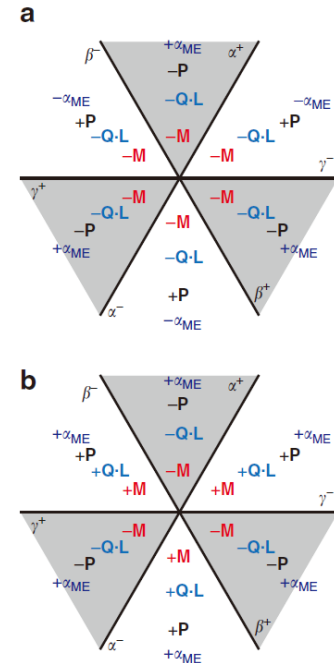
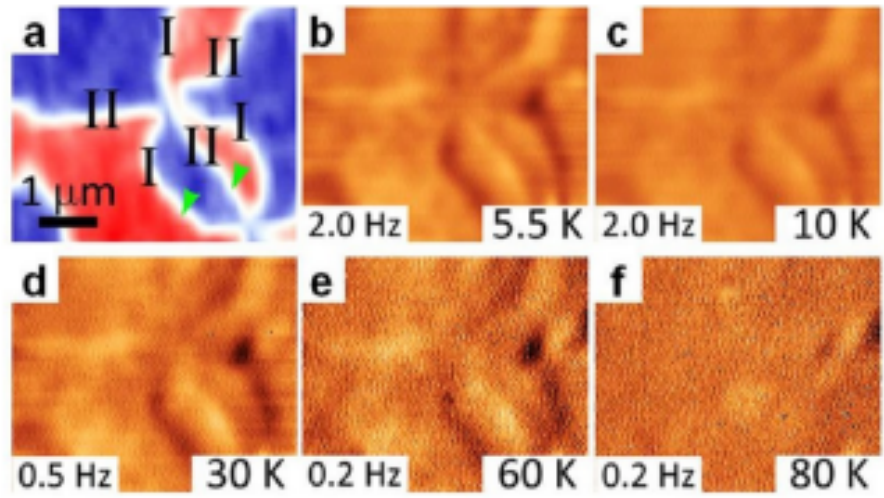
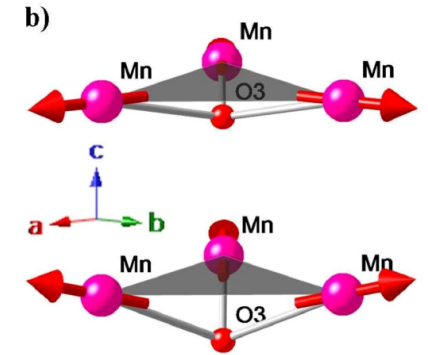
4 possible magnetic structure of P6<sub>3</sub>cm space group





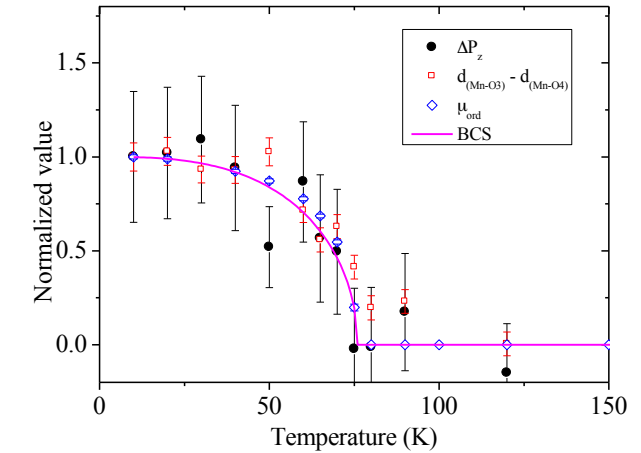
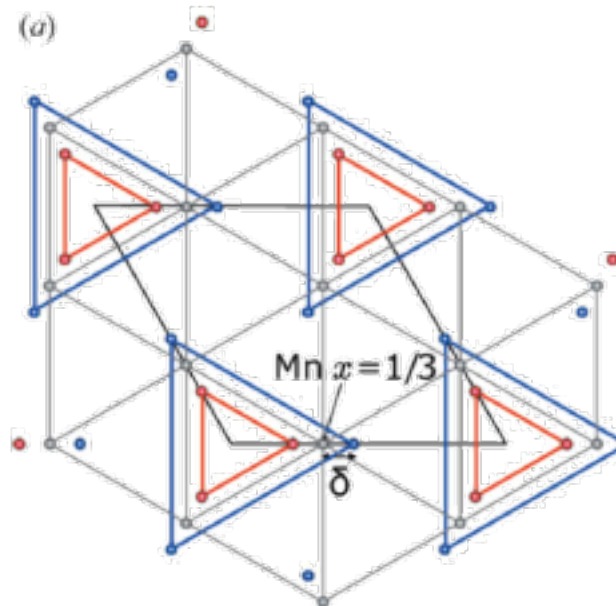
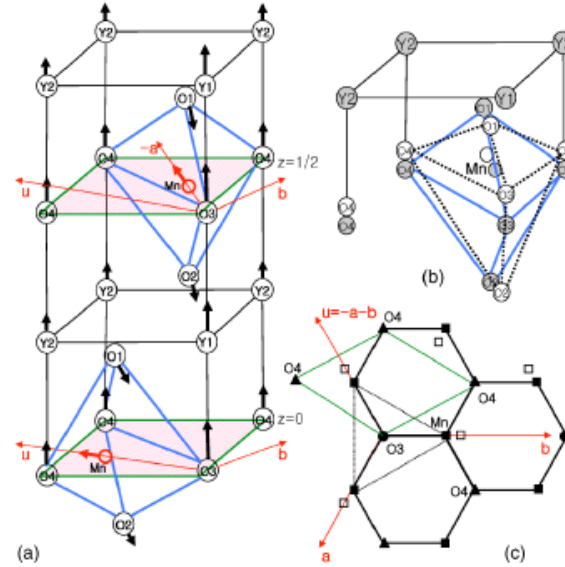
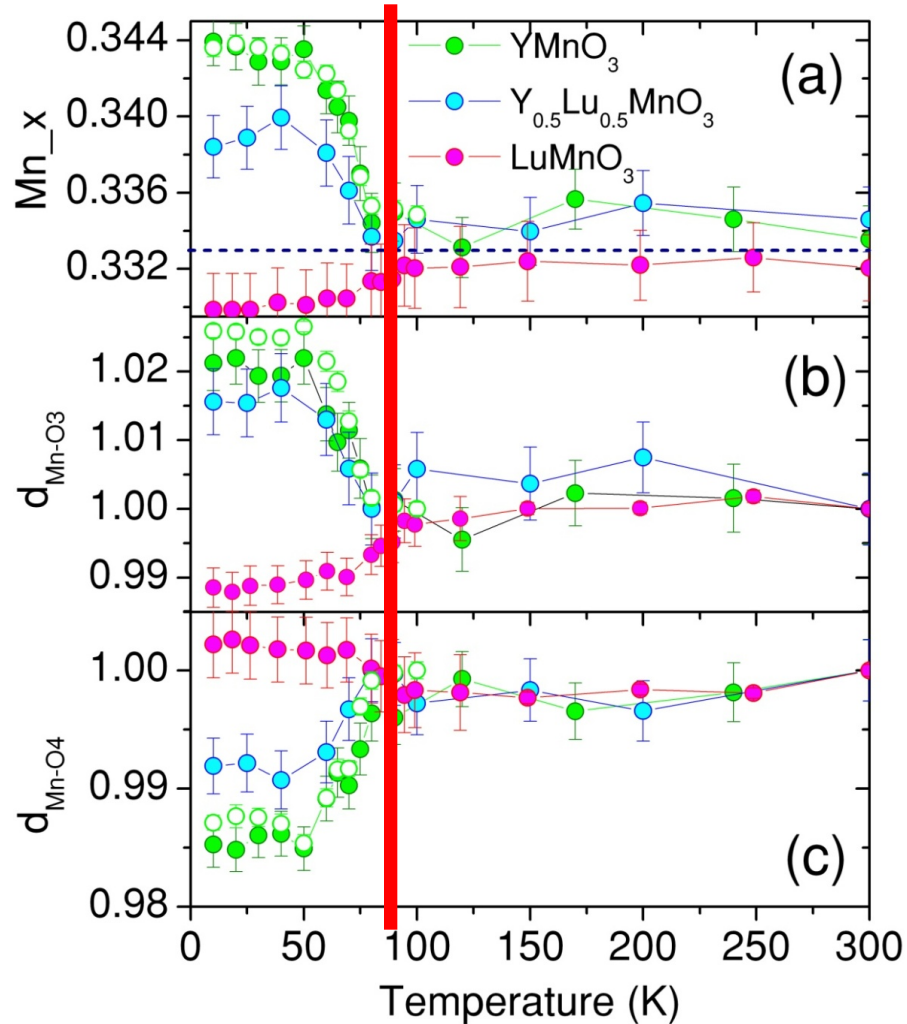


$Q_{K_3}$  phonon mode (Ferroelectric transition)



Several papers from S-W Cheong's group  
 Y. Geng et al., Nano Lett., 12, 6055 (2012)  
 H. Das et al., Nat. Commun. 5, 2998 (2014)

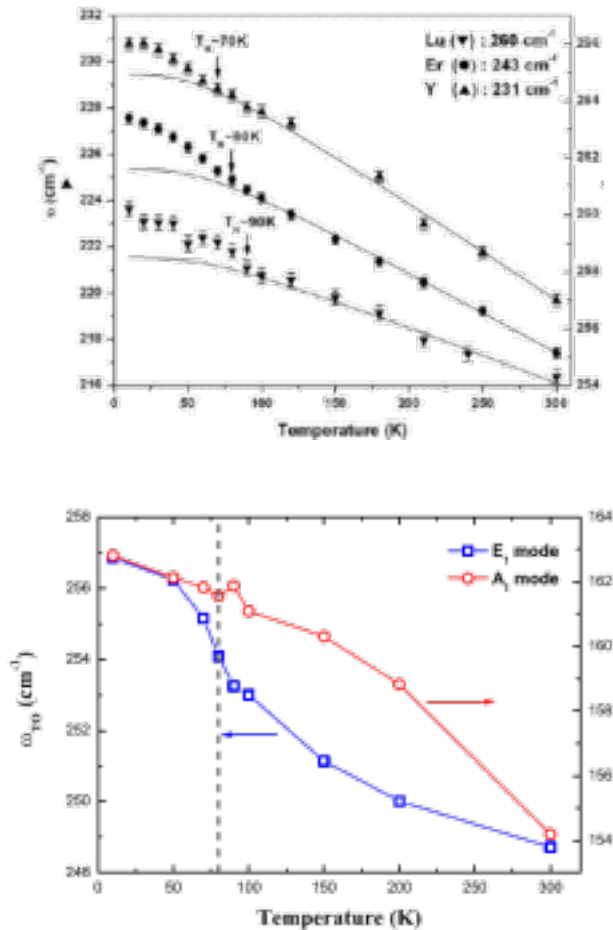
- Atomic displacement below  $T_N$
- Large displacement of Mn x position induces Mn trimerization.



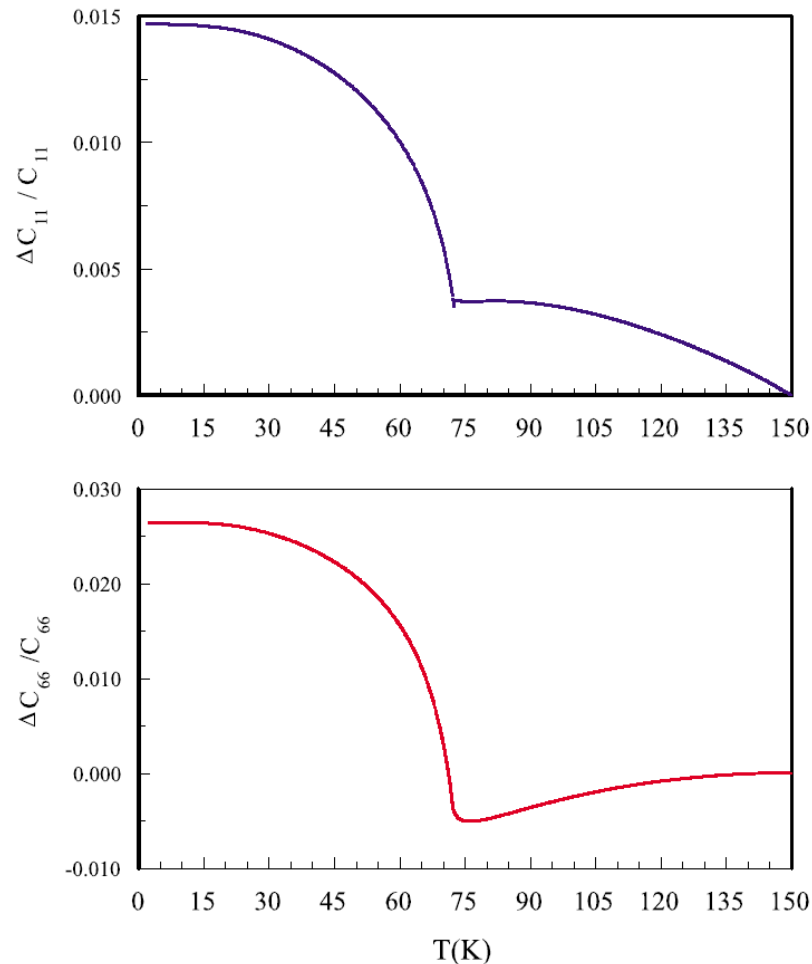
$$\Delta \vec{P}(T) = \sum_i q_i (\vec{r}_i(T) - \vec{r}_i(300K)),$$

- Numerous evidences of spin-lattice(phonon) coupling in YMnO<sub>3</sub>

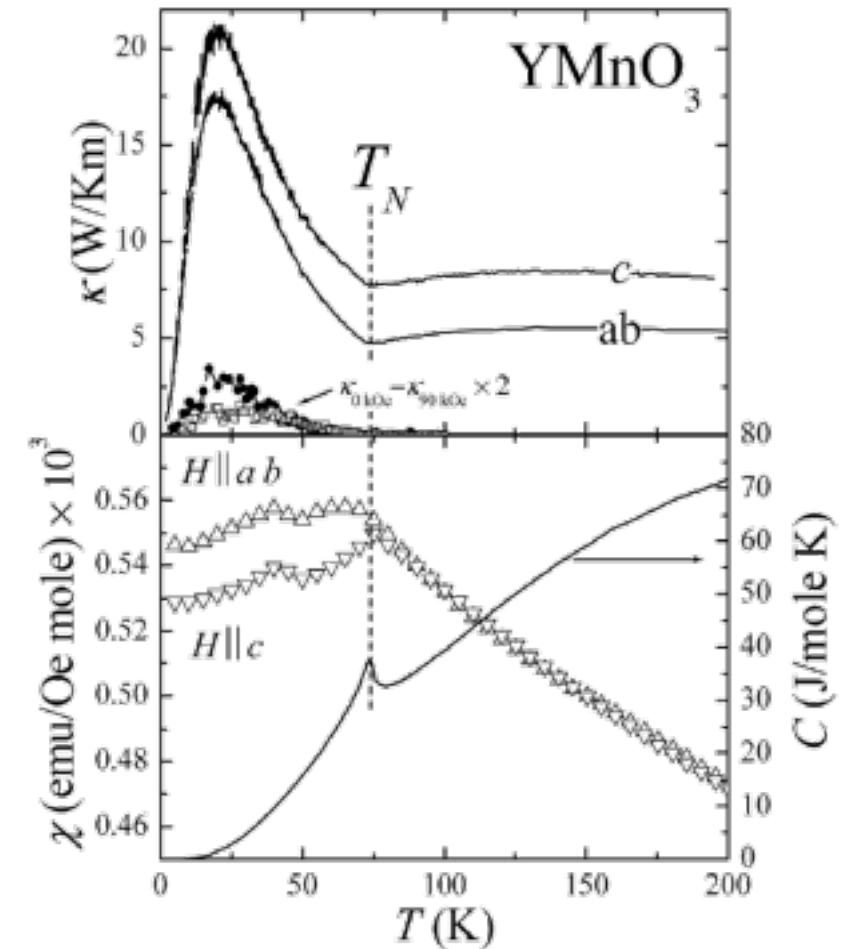
Phonon anomaly



Elastic moduli



Thermal conductivity

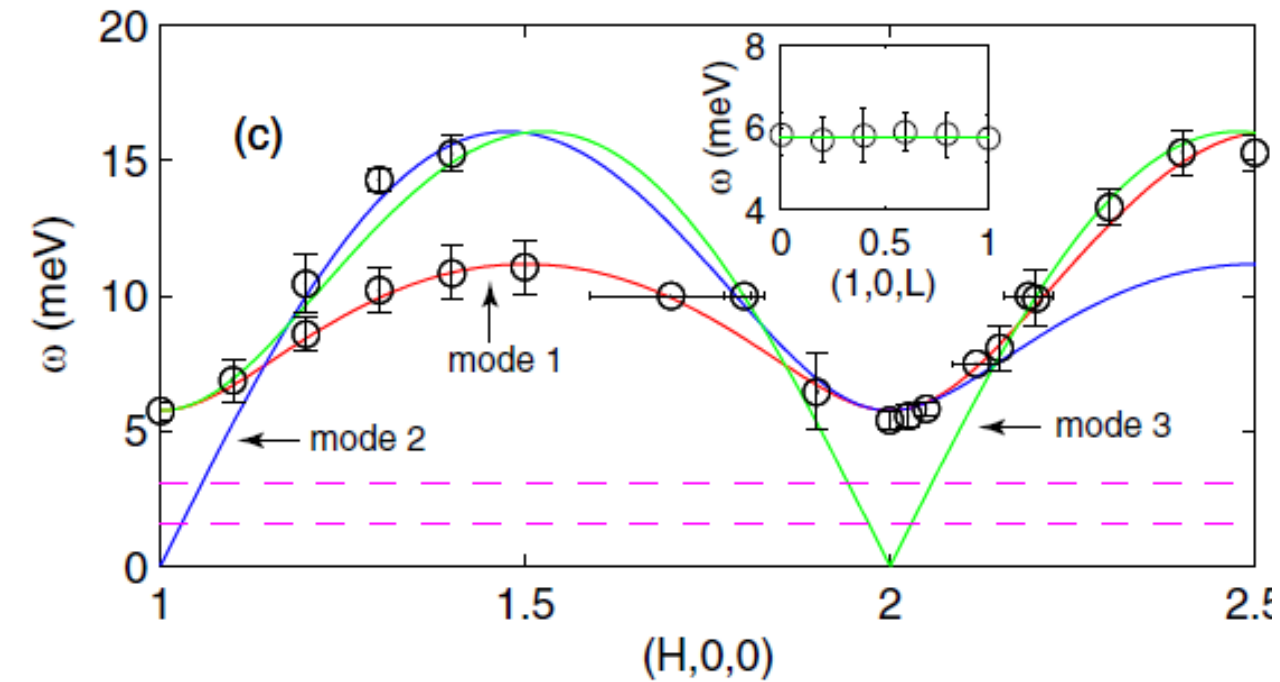


- Three magnon modes
- $J=2.5$  meV,  $D=0.28$  meV

## Spin Hamiltonian

$$H_{ex} = J \sum_{\langle r, r+\delta \rangle} S_r \cdot S_{r+\delta} + D \sum_r (S_r^z)^2$$

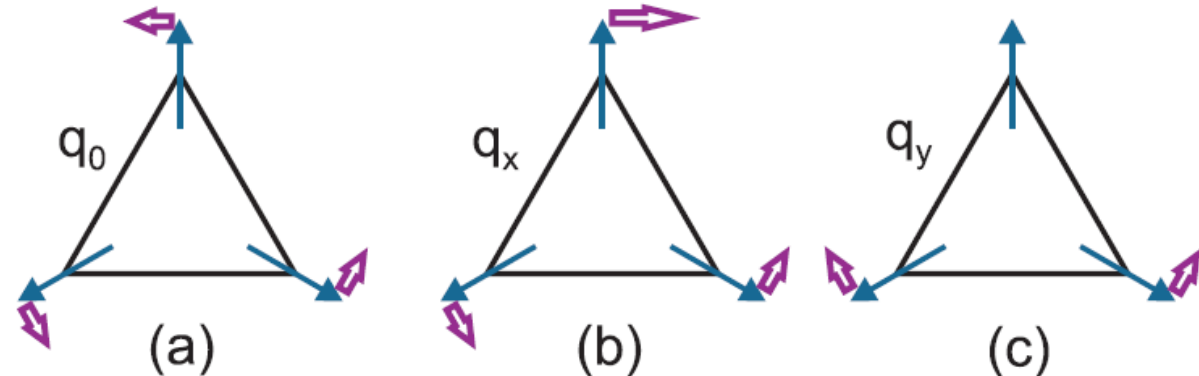
Antiferro
Easy plane  
 $J > 0$ 
 $D > 0$



O. P. Vajk *et al.*, PRL **94**, 087601 (2005)

Phason mode  
(mode 1)

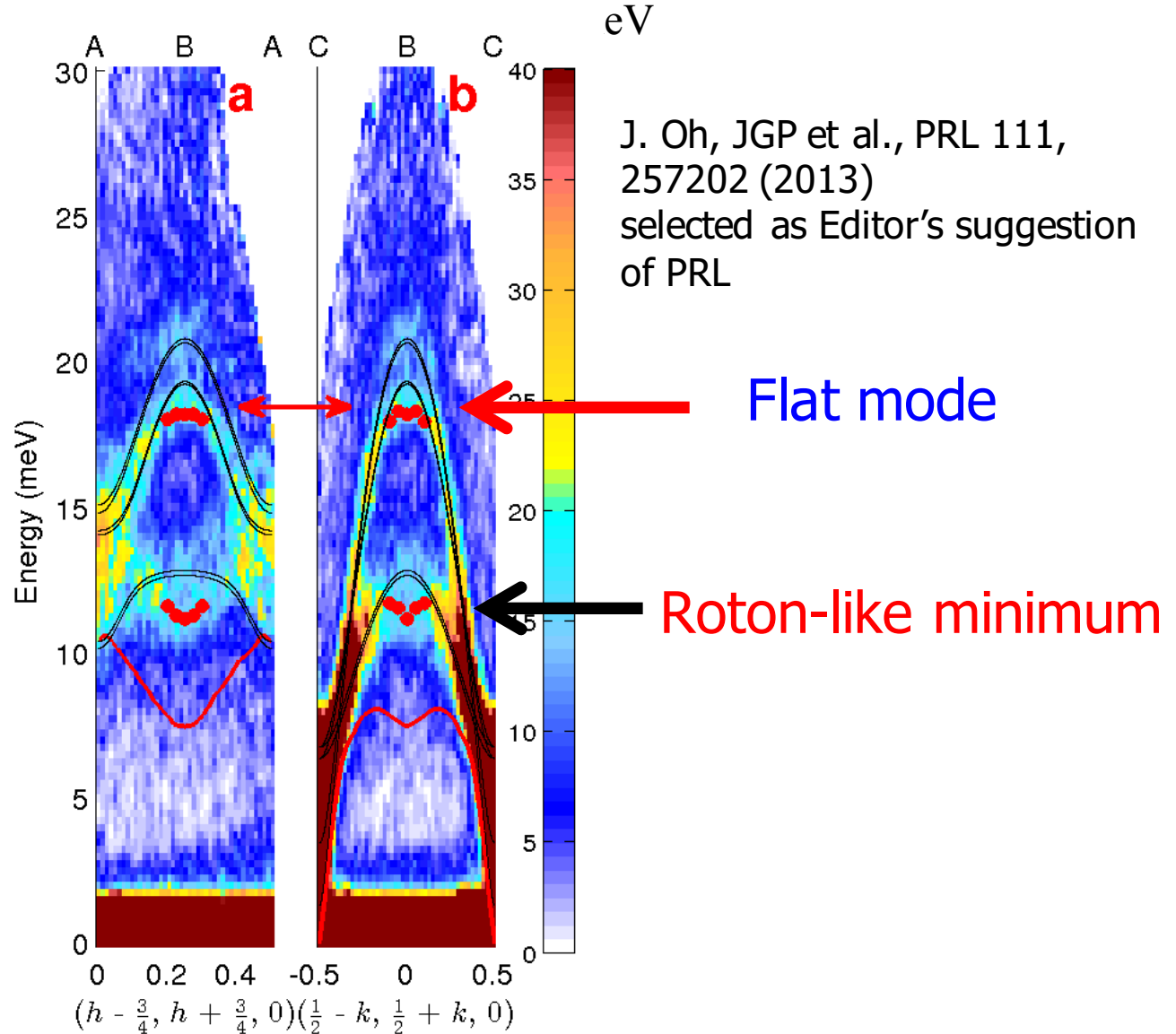
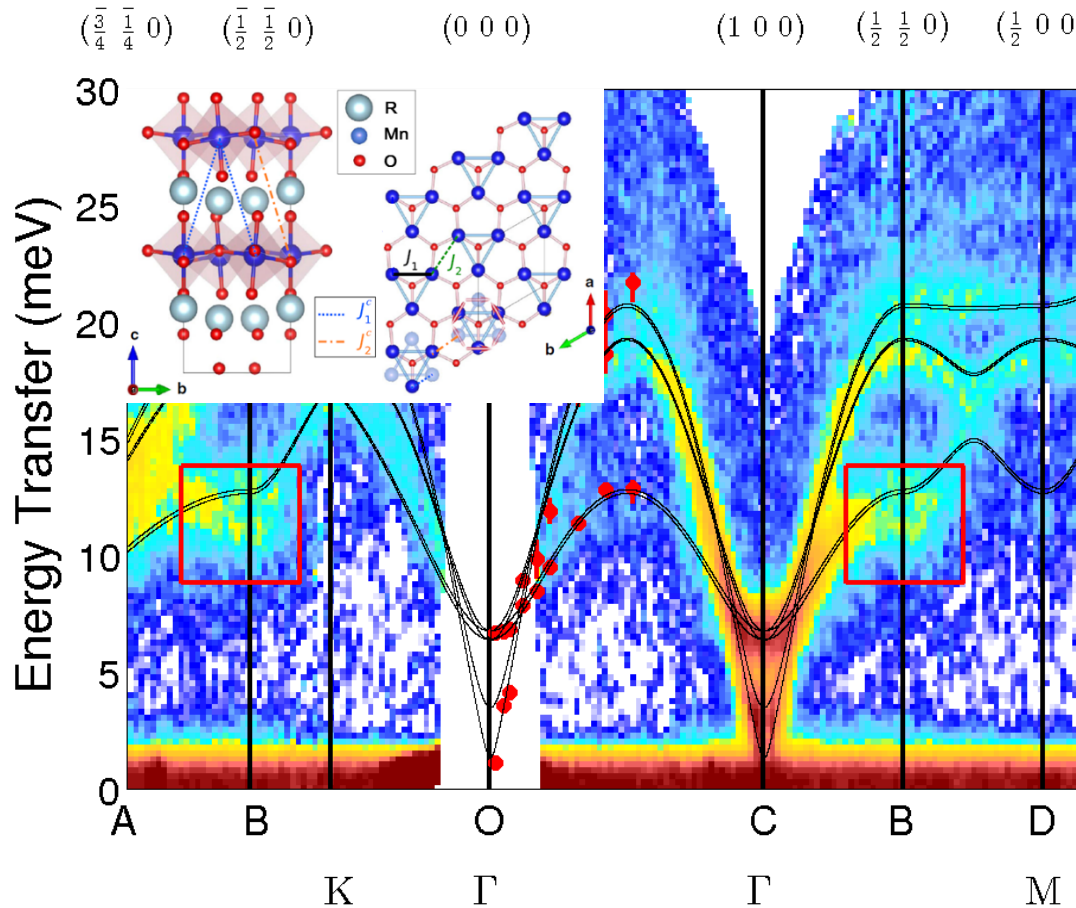
Spin canting modes  
(mode 2,3)



M. A. van der Varte *et al.*, arXiv:0907.3055

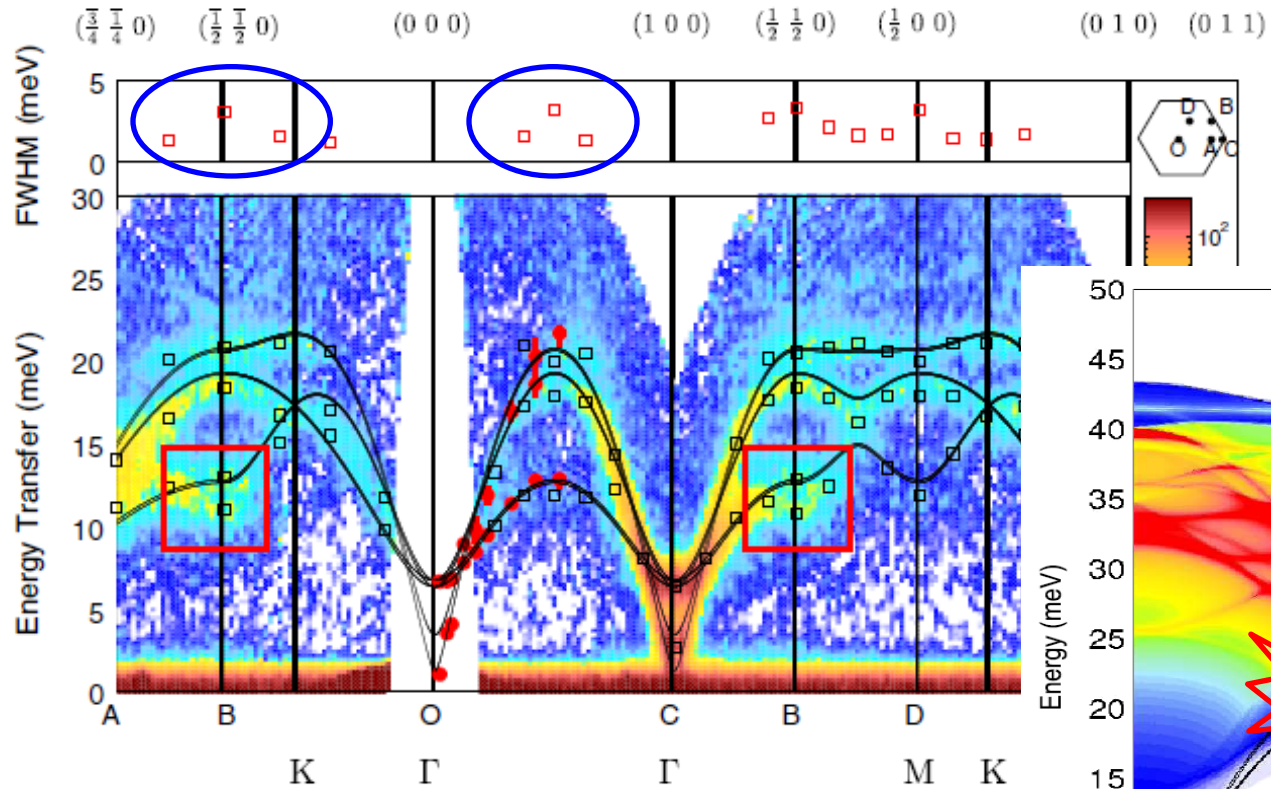
$$H = -J_1 \sum_{\text{intra}} \vec{S}_i \vec{S}_j - J_2 \sum_{\text{inter}} \vec{S}_i \vec{S}_j - J_1' \sum_{\text{out intra}} \vec{S}_i \vec{S}_j - J_2' \sum_{\text{out inter}} \vec{S}_i \vec{S}_j - J_3 \sum_{\text{next nn}} \vec{S}_i \vec{S}_j - D_1 \sum (S_i^z)^2 - D_2 \sum (\vec{n} \cdot \vec{S}_i)^2$$

$J_1 = -9 \text{ meV}, J_2 = -1.4 \text{ meV}, J_3 = 0 \text{ meV}, J_1' = -0.018 \text{ meV}$

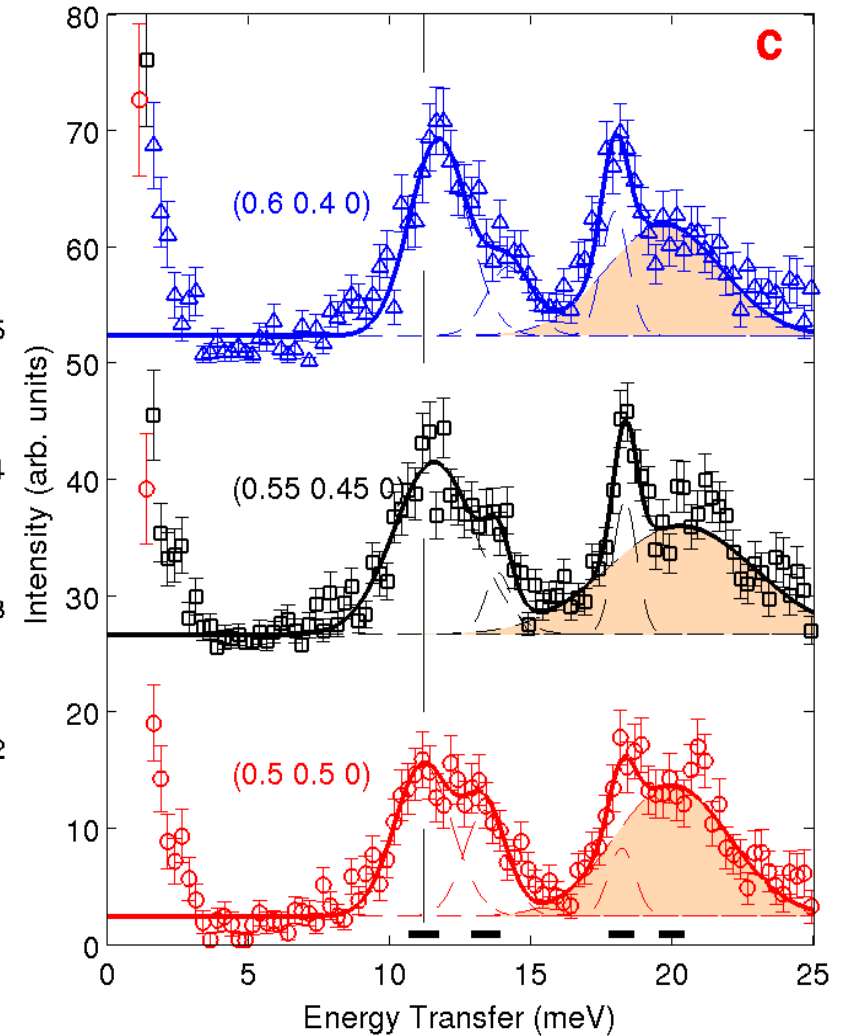
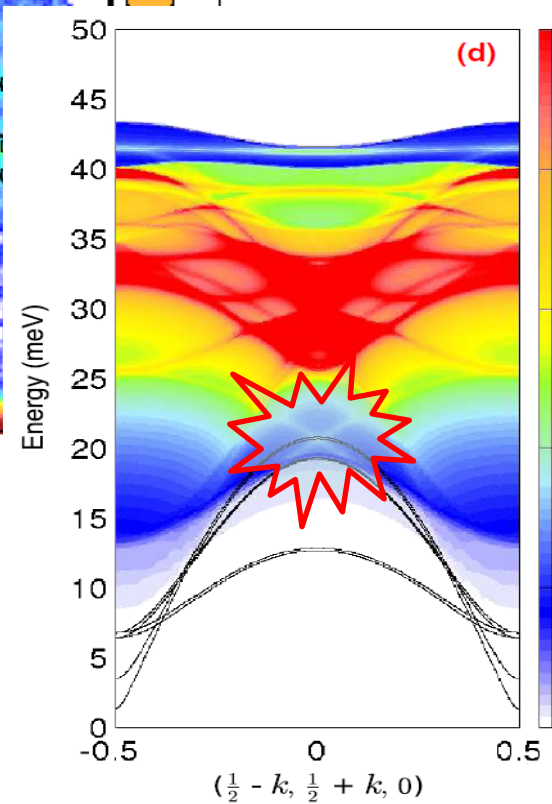


## Observation of linewidth broadening in $\text{LuMnO}_3$

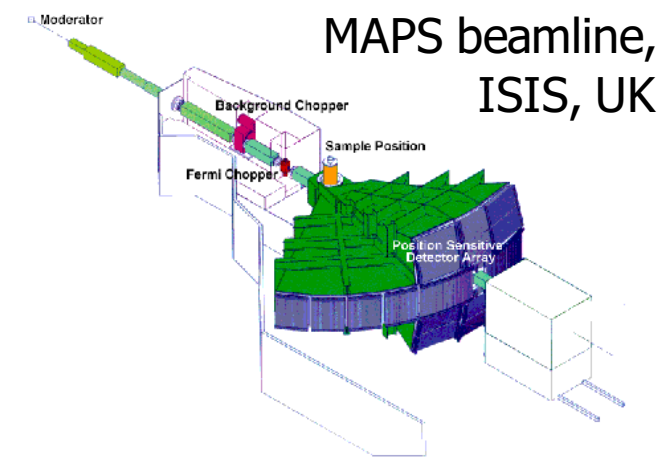
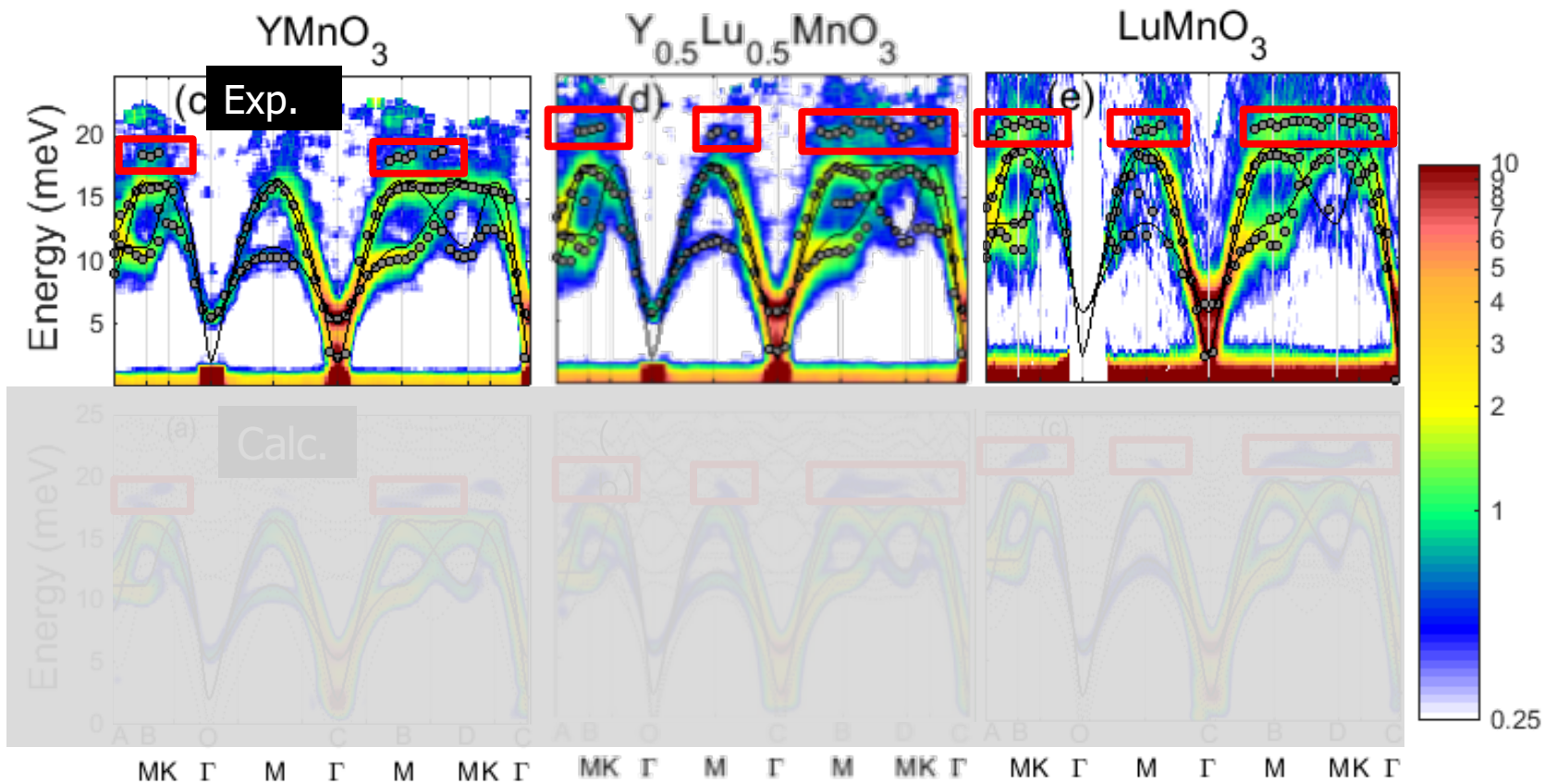
J. Oh, JGP et al., PRL 111, 257202 (2013)  
 selected as Editor's suggestion of PRL



Two magnons DOS



$$H = H_{spin} + H_{phonon} - \alpha' \sum_{\langle ij \rangle} (e_{o_{ij}i} \cdot u_i + e_{o_{ij}j} u_j) S_i \cdot S_j$$



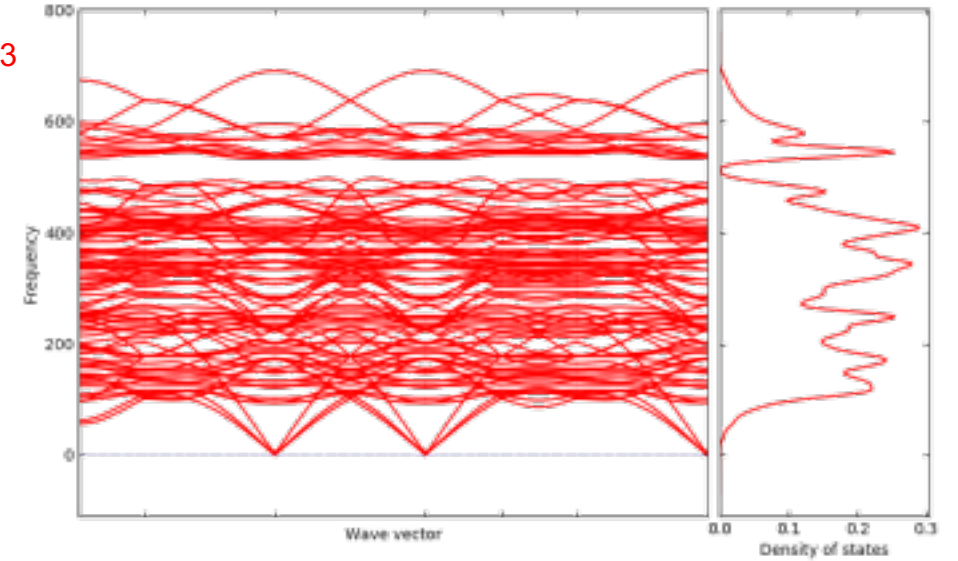
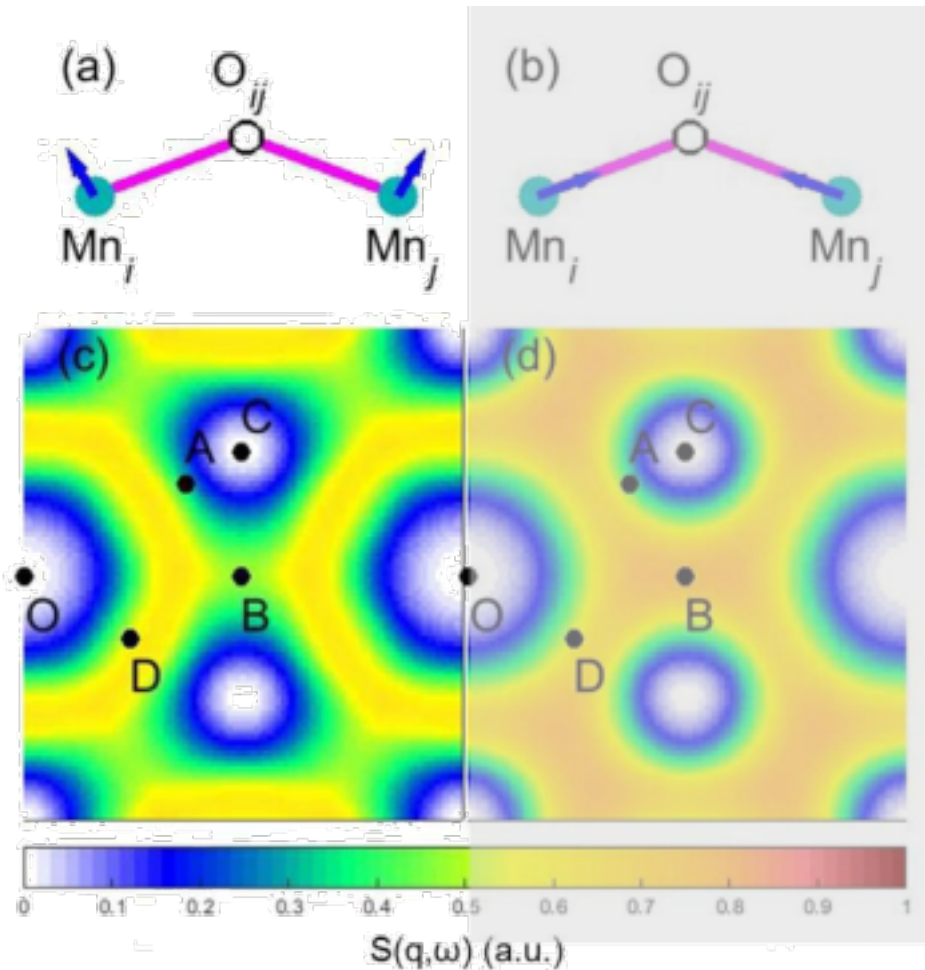
Magneto-phonon mode

Joosung Oh

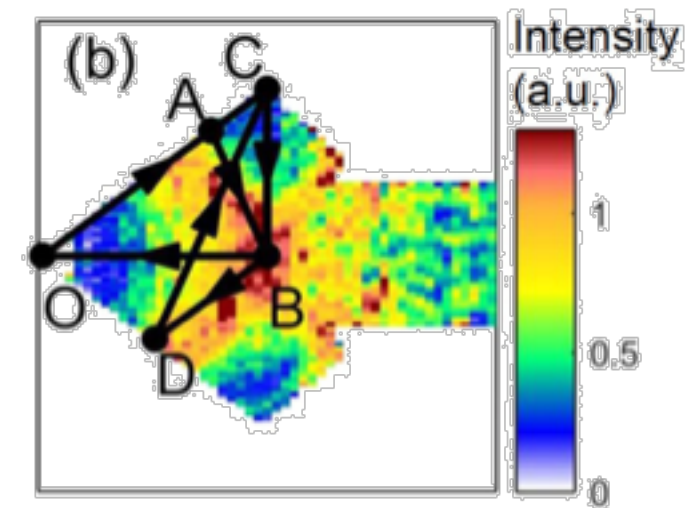


Mn-O Bond-length change is dominant for exchange-striction in YMnO<sub>3</sub>

$$H = H_{spin} + \hbar \sum_{i=1}^{90} \omega_i b_k^\dagger b_k + \frac{\alpha J}{2d} \sum_{ij} (e_{o_{ij}i} \cdot \mathbf{U}_i + e_{o_{ij}j} \cdot \mathbf{U}_j) \mathbf{S}_i \cdot \mathbf{S}_j$$



DFT phonon result of YMnO<sub>3</sub>

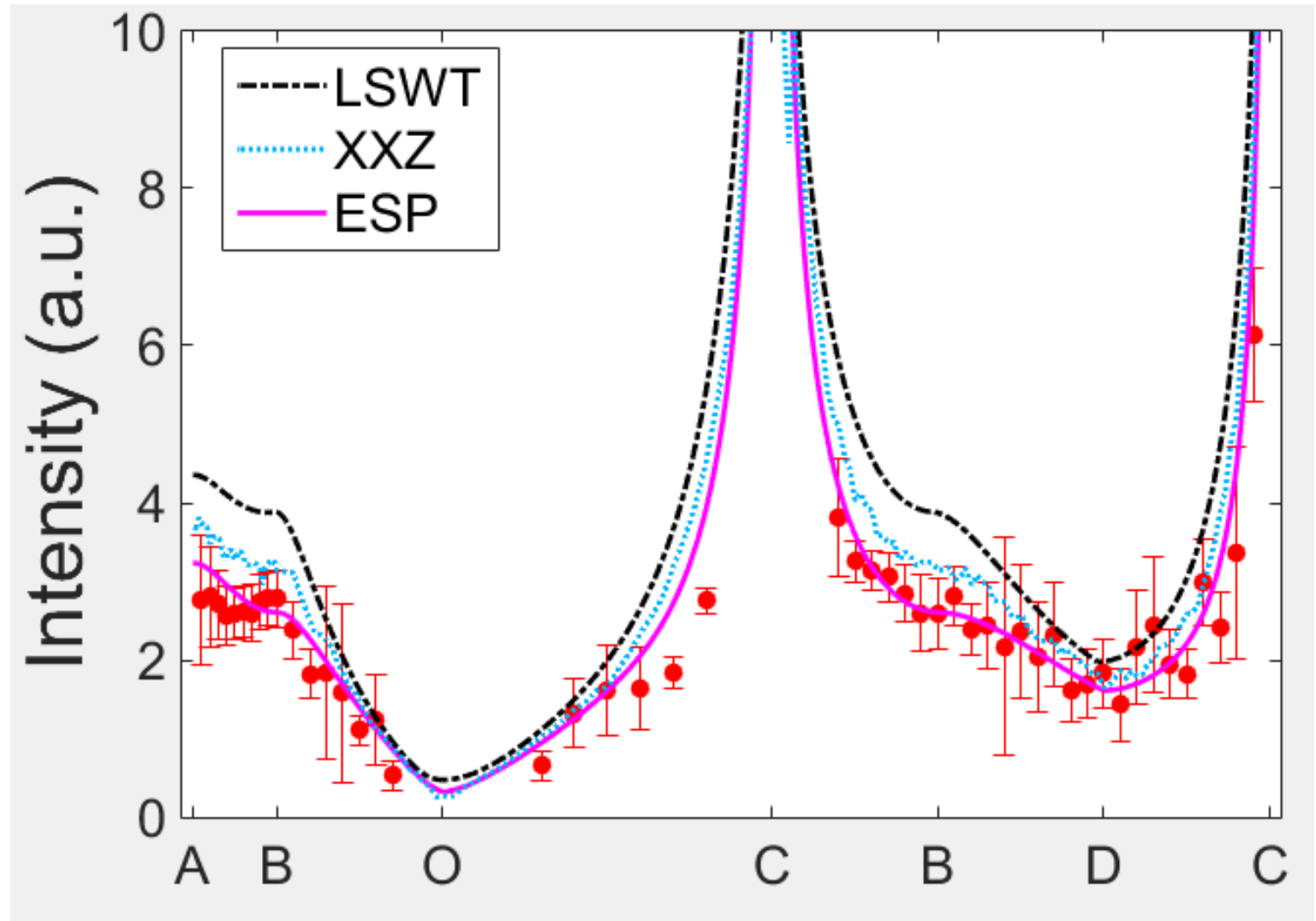
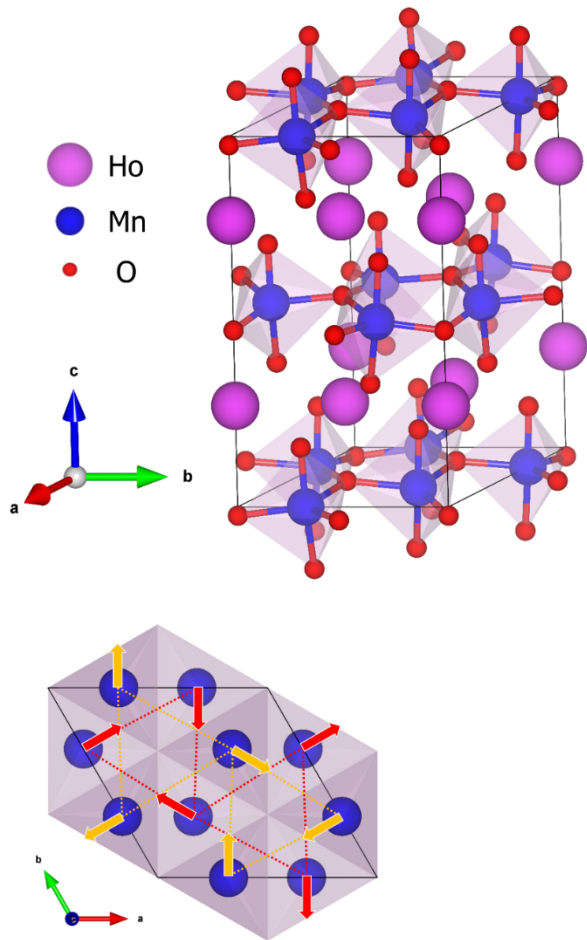


INS Dynamical Structure Factor





Taehun Kim, JGP et al.,  
Phys. Rev. B 97, 201113(R)  
(2018)



Overall features are all similar for all three different models although the ESP model is slightly better.

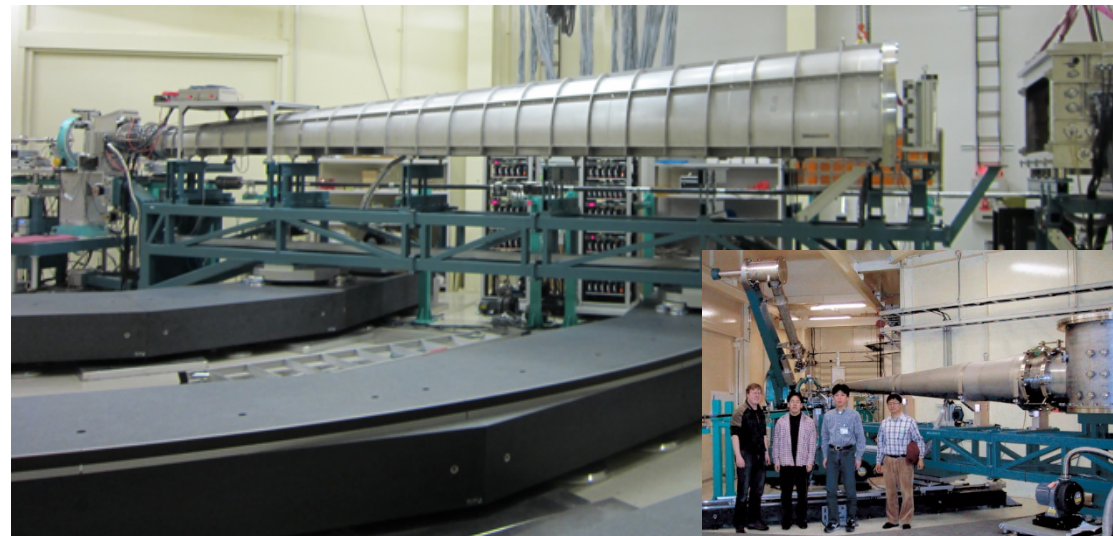
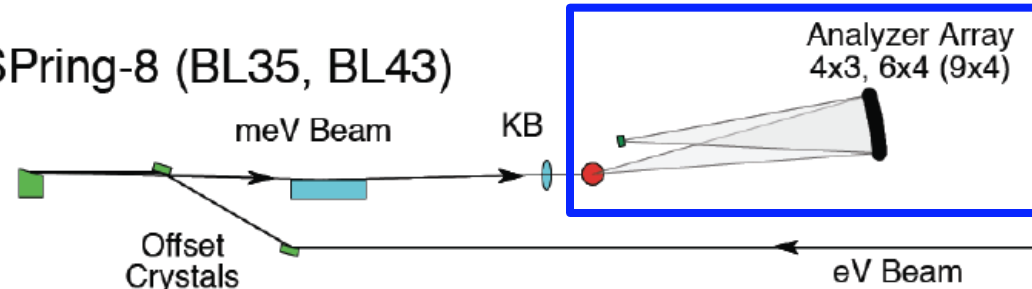
## BL 43XU at Spring-8, Japan

- Simultaneous measurement of 24 different q points
- q & E resolution:  $0.05 \text{ \AA}^{-1}$  & 1.5 meV

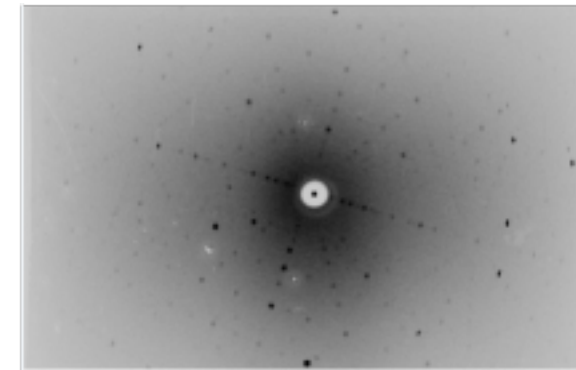
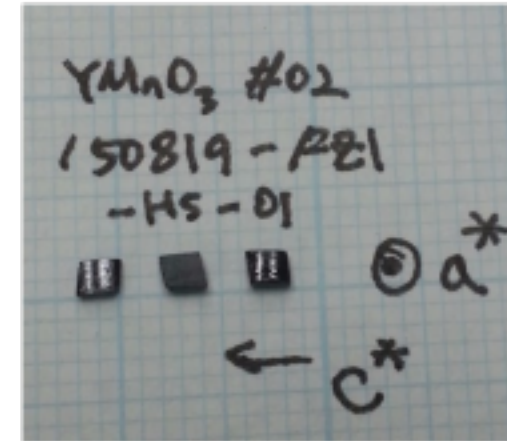
Main Operating Conditions at BL43LXU

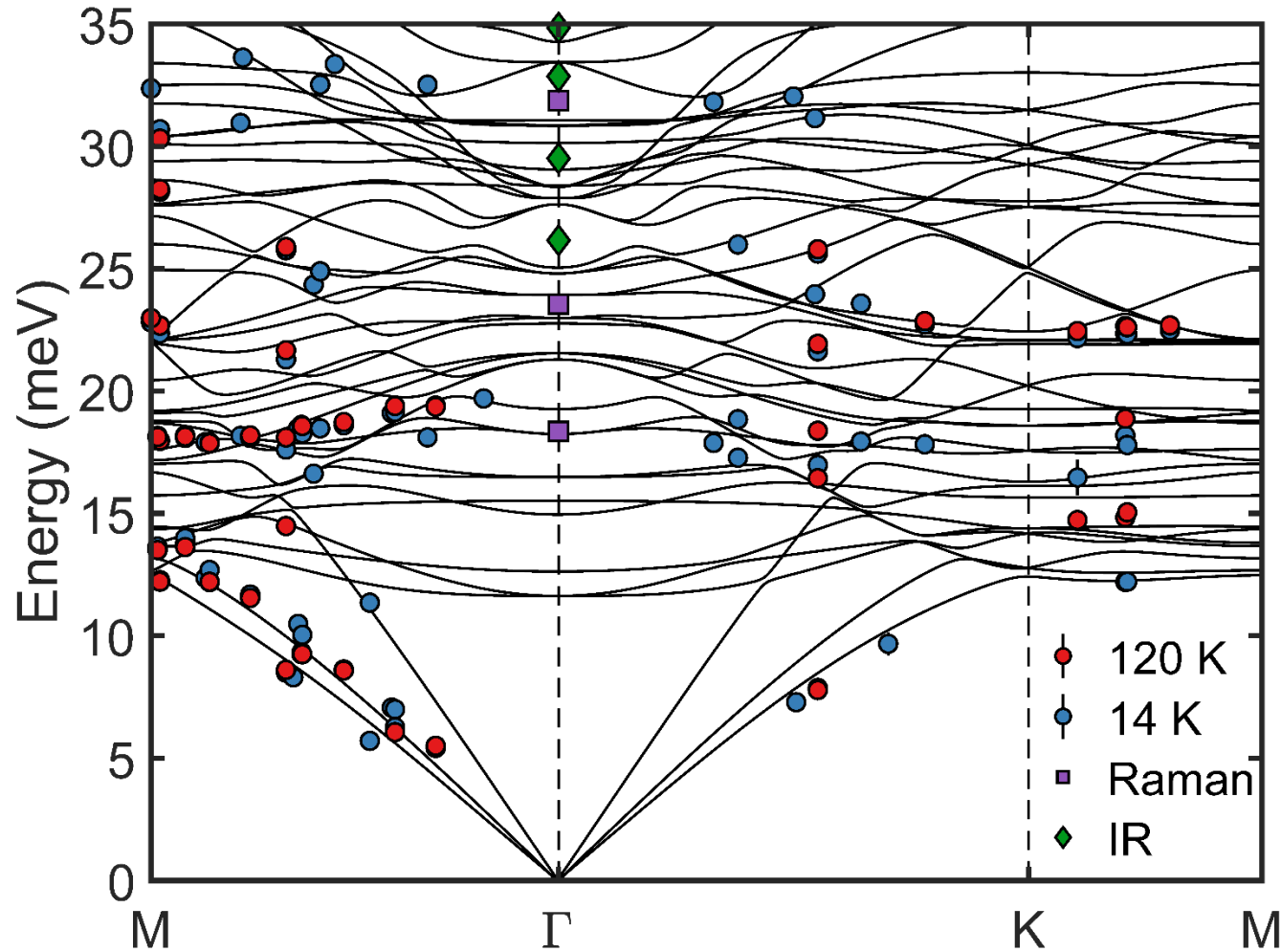
| Spectrometer                                     | High Resolution (Atomic Dynamics)   |            |         |         |
|--|---|------------|---------|---------|
|  | 25.70   | 21.75      | 17.79   | 15.82   |
| X-ray Energy (keV)                               | 25.70   | 21.75      | 17.79   | 15.82   |
| Energy Resolution FWHM (meV)                     | >0.75   | >1.25      | >2.8    | ~6      |
| Analyzer Reflection Si (nnn)                     | (13 13 13)  | (11 11 11) | (9 9 9) | (8 8 8) |
| Maximum Momentum Transfer ( $\text{\AA}^{-1}$ )  | 12  | 10         | 8.3     | 7.4     |
| Photons at the Sample (Relative: 1 unit ~25 GHz) | ~0.2  | ~1         | ~3      | ~10     |
| Analyzer Solid Angle                             | ~ $0.2 \times 0.2 \text{ mrad}^2$ (Min.) to $9.4 \times 8.9 \text{ mrad}^2$ (HxV, Max.) |            |         |         |
| Beam Size at Sample Diameter, FWHM               | ~50 $\mu\text{m}$ (Default), ~15 $\mu\text{m}$ (Compound Focus)                         |            |         |         |

(b) SPring-8 (BL35, BL43)



Kisoo Park

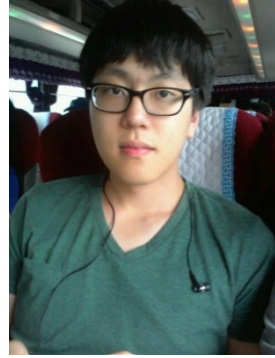




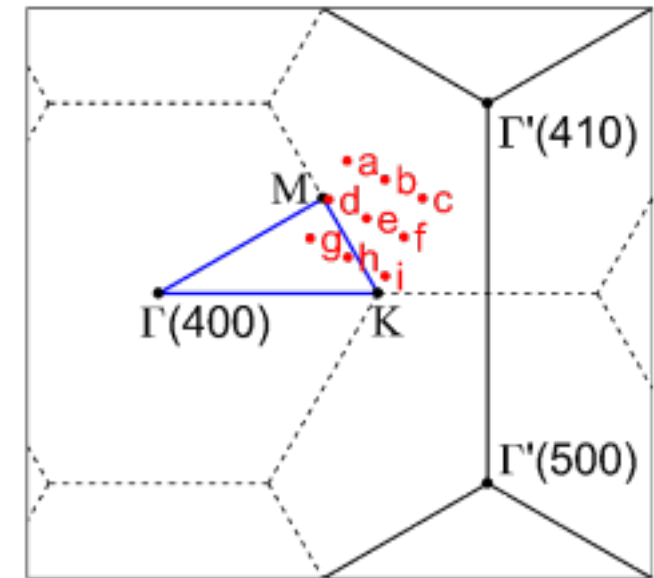
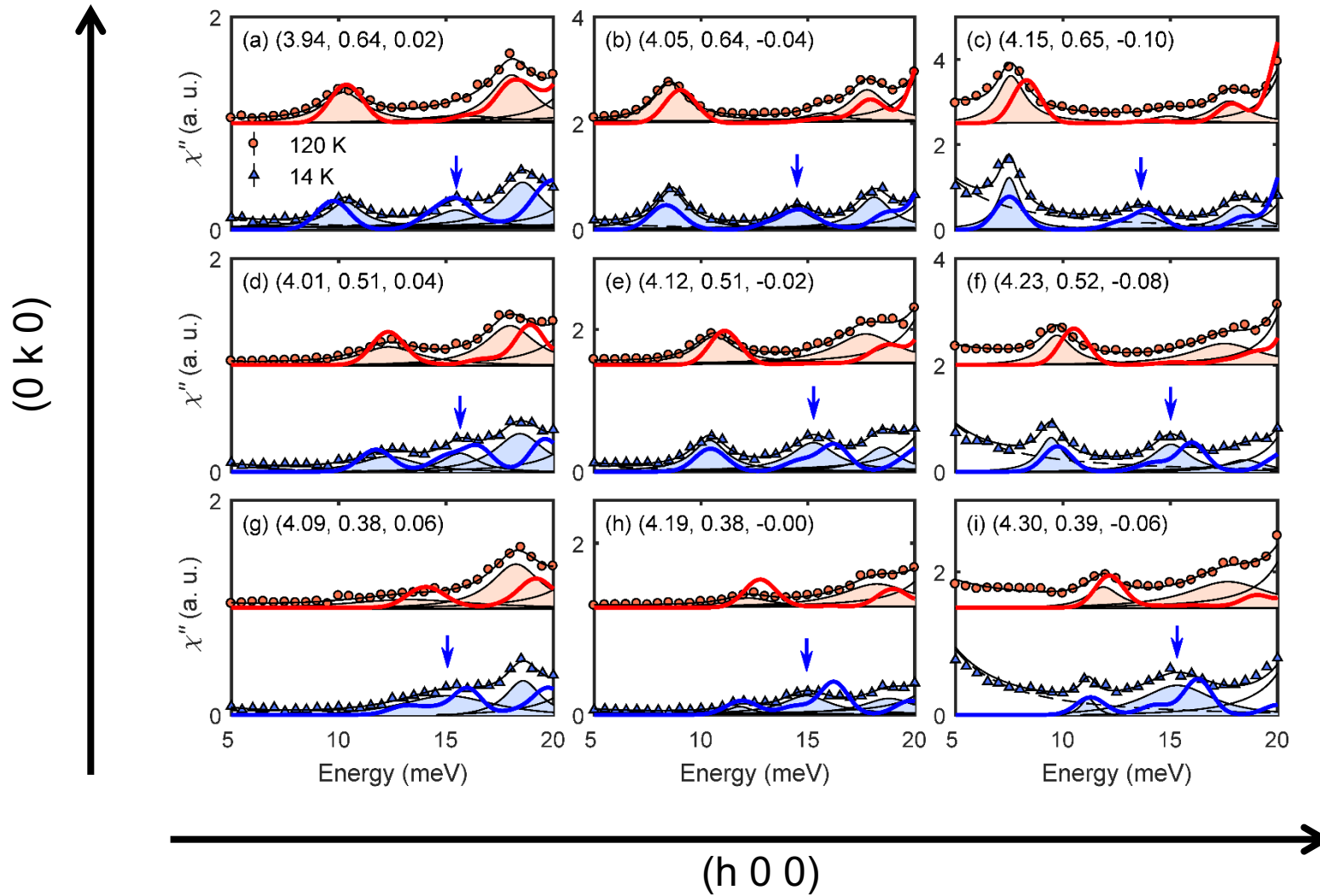
## Key Observations

- We have succeeded in measuring several key phonons by using inelastic X-ray scattering technique.
- We have also found a significant shift induced by cooling.

K. Park, J.-G. Park et al., in preparation



Kiso Park



Red: HT (120 K)  
Blue: LT (14 K)

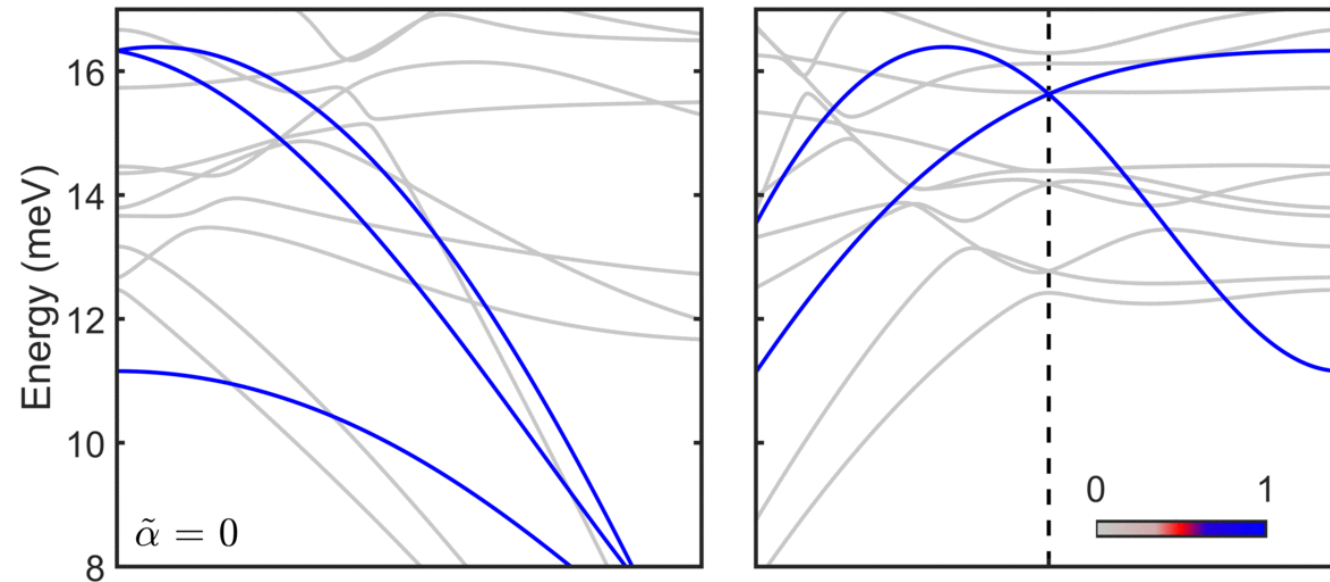
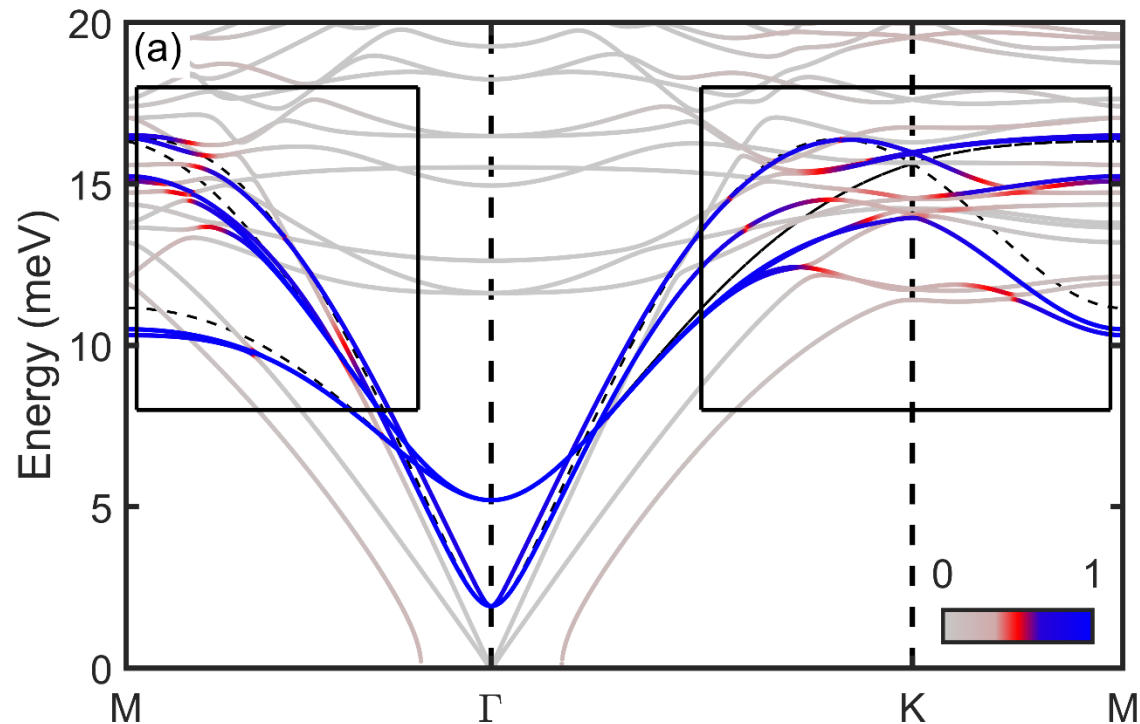
Each magneto-elastic modes can be characterized by the ratio between magnon/phonon components

$$(p_i^{mag}(\mathbf{q}) + p_i^{ph}(\mathbf{q}) = 1, \quad p_i^{mag/ph}(\mathbf{q}): \text{magnon/phonon character of } i\text{-th band at } \mathbf{q} \text{ point}).$$

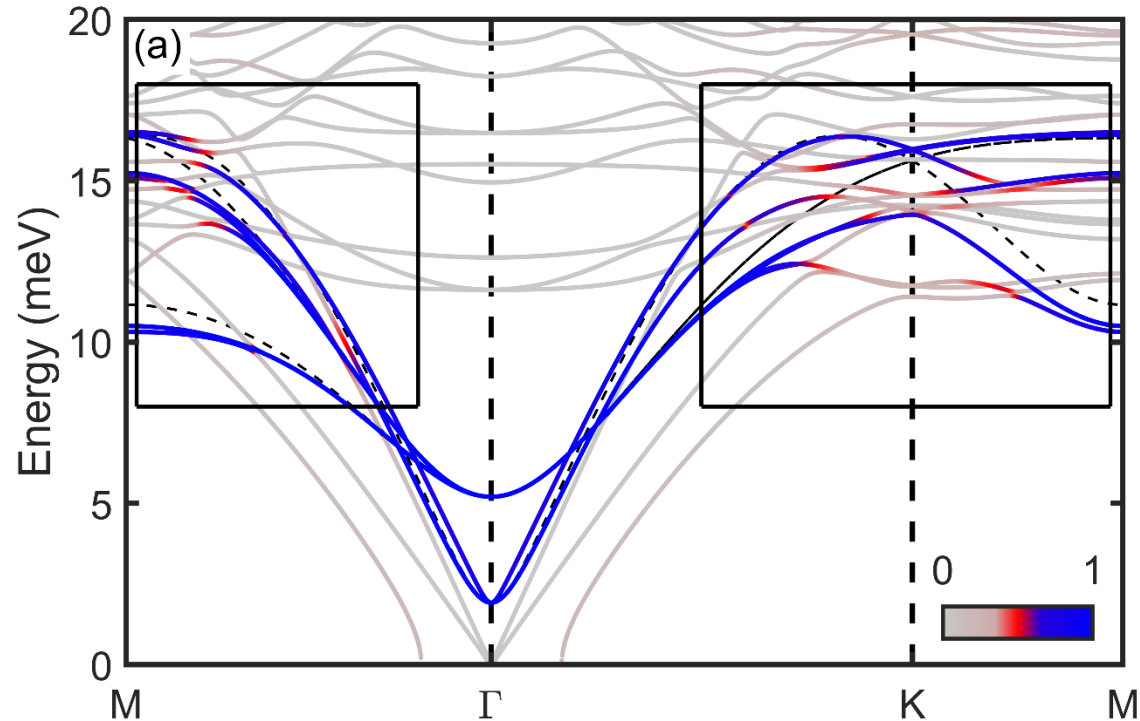
Magneto-elastic modes colored with the magnon character  $p_i^{mag}(\mathbf{q})$

**96×96 Matrix**

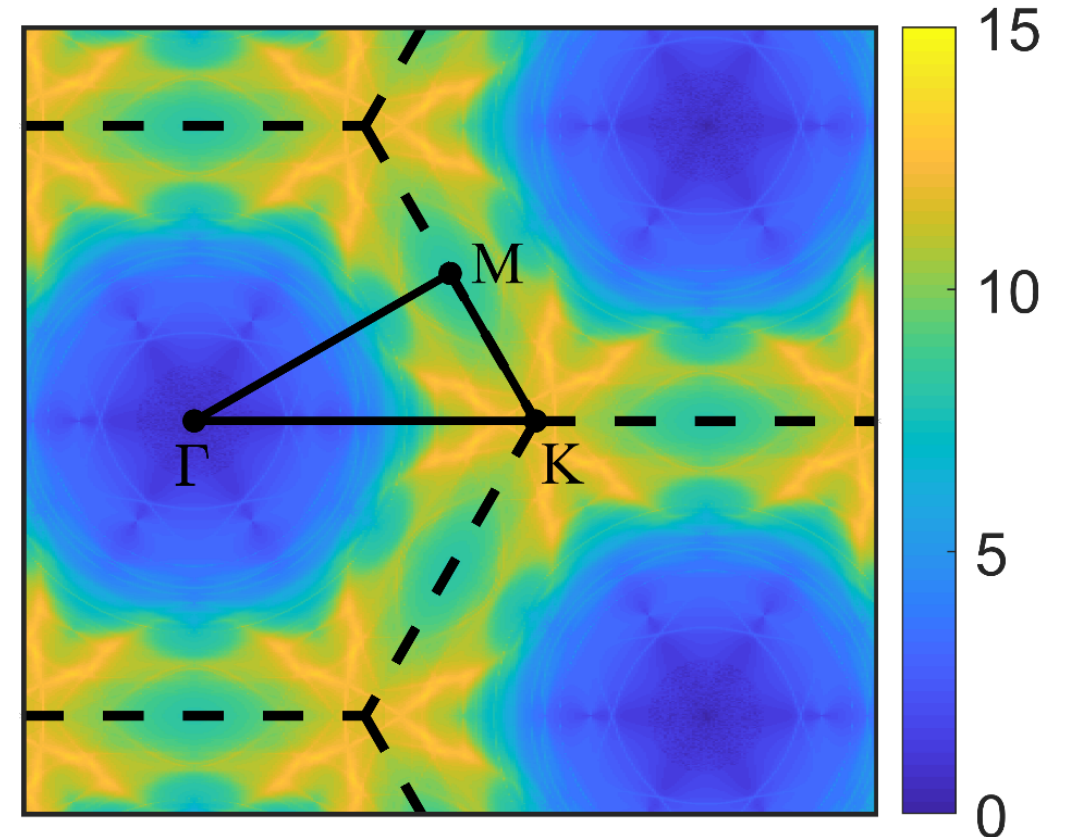
Matrix from:  $H = S \sum_k X_{tot}^\dagger \begin{pmatrix} L & -iN^\dagger & M & -iN^\dagger \\ iN & \Omega & -iN & 0 \\ M & iN^\dagger & L & -iN^\dagger \\ iN & 0 & iN & \Omega \end{pmatrix} X_{tot}$



- Each magneto-elastic modes can be characterized by the ratio between magnon/phonon components ( $p_i^{mag}(\mathbf{q}) + p_i^{ph}(\mathbf{q}) = 1$ ,  $p_i^{mag/ph}(\mathbf{q})$ : magnon/phonon character of  $i$ -th band at  $\mathbf{q}$  point).
- We can define the 'magnon-phonon mixing entropy'  $S(\mathbf{q}) = -\sum_i p_i^{mag}(\mathbf{q}) \log(p_i^{mag}(\mathbf{q}))$  to quantify the mode-integrated momentum dependence of magnon-phonon coupling.



Magnon-Phonon Mixing Entropy



We can diagonalize pure magnon Hamiltonian in MP-coupled Hamiltonian.

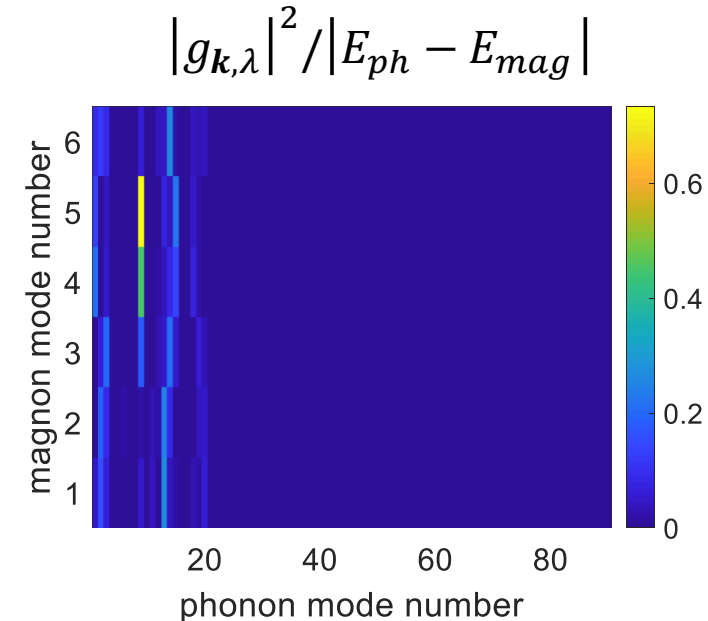
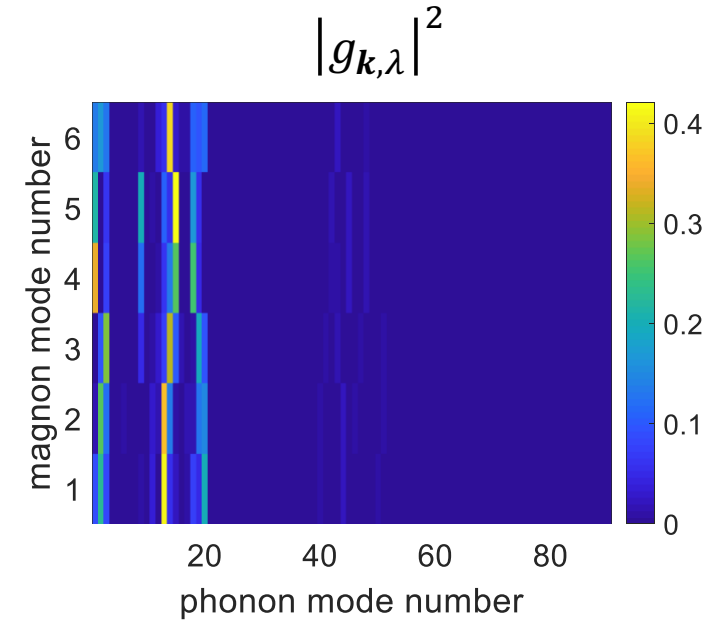
$$\mathcal{H}_{mag}(\mathbf{k}) = \begin{pmatrix} A_{\mathbf{k}} & B_{\mathbf{k}} \\ B_{\mathbf{k}} & A_{\mathbf{k}} \end{pmatrix}, \quad \mathcal{H}_{mp}(\mathbf{k}) = \begin{pmatrix} A_{\mathbf{k}} & N_{\mathbf{k},\lambda}^{\dagger} & B_{\mathbf{k}} & N_{\mathbf{k},\lambda} \\ N_{\mathbf{k},\lambda} & E_{ph}(\mathbf{k},\lambda) & N_{\mathbf{k},\lambda}^{\dagger} & 0 \\ B_{\mathbf{k}} & N_{\mathbf{k},\lambda} & A_{\mathbf{k}} & N_{\mathbf{k},\lambda}^{\dagger} \\ N_{\mathbf{k},\lambda}^{\dagger} & 0 & N_{\mathbf{k},\lambda} & E_{ph}(\mathbf{k},\lambda) \end{pmatrix}$$

where  $V_{mag}^{\dagger} \cdot \mathcal{H}_{mag}(\mathbf{k}) \cdot V_{mag} = E_{mag}$ ,  $V_{mag} = \begin{pmatrix} \alpha_{\mathbf{k}} & \beta_{\mathbf{k}} \\ \gamma_{\mathbf{k}} & \delta_{\mathbf{k}} \end{pmatrix}$

$$\rightarrow \begin{pmatrix} \alpha_{\mathbf{k}} & 0 & \beta_{\mathbf{k}} & 0 \\ 0 & I & 0 & 0 \\ \gamma_{\mathbf{k}} & 0 & \delta_{\mathbf{k}} & 0 \\ 0 & 0 & 0 & I \end{pmatrix}^{\dagger} \cdot \begin{pmatrix} A_{\mathbf{k}} & N_{\mathbf{k},\lambda}^{\dagger} & B_{\mathbf{k}} & N_{\mathbf{k},\lambda} \\ N_{\mathbf{k},\lambda} & E_{ph}(\mathbf{k},\lambda) & N_{\mathbf{k},\lambda}^{\dagger} & 0 \\ B_{\mathbf{k}} & N_{\mathbf{k},\lambda} & A_{\mathbf{k}} & N_{\mathbf{k},\lambda}^{\dagger} \\ N_{\mathbf{k},\lambda}^{\dagger} & 0 & N_{\mathbf{k},\lambda} & E_{ph}(\mathbf{k},\lambda) \end{pmatrix} \cdot \begin{pmatrix} \alpha_{\mathbf{k}} & 0 & \beta_{\mathbf{k}} & 0 \\ 0 & I & 0 & 0 \\ \gamma_{\mathbf{k}} & 0 & \delta_{\mathbf{k}} & 0 \\ 0 & 0 & 0 & I \end{pmatrix}$$

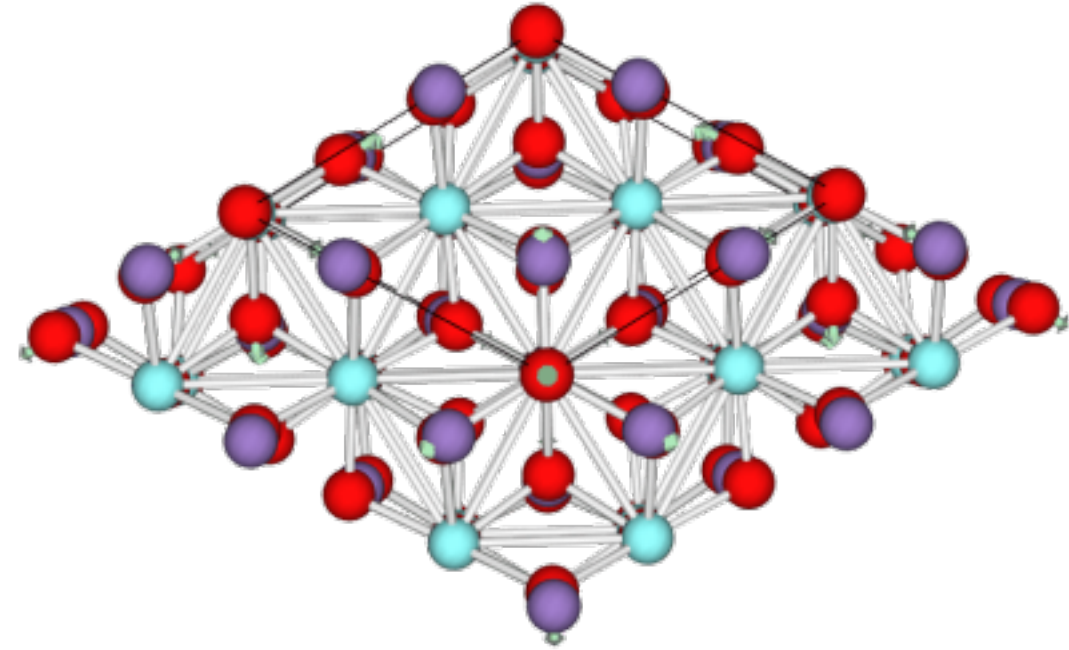
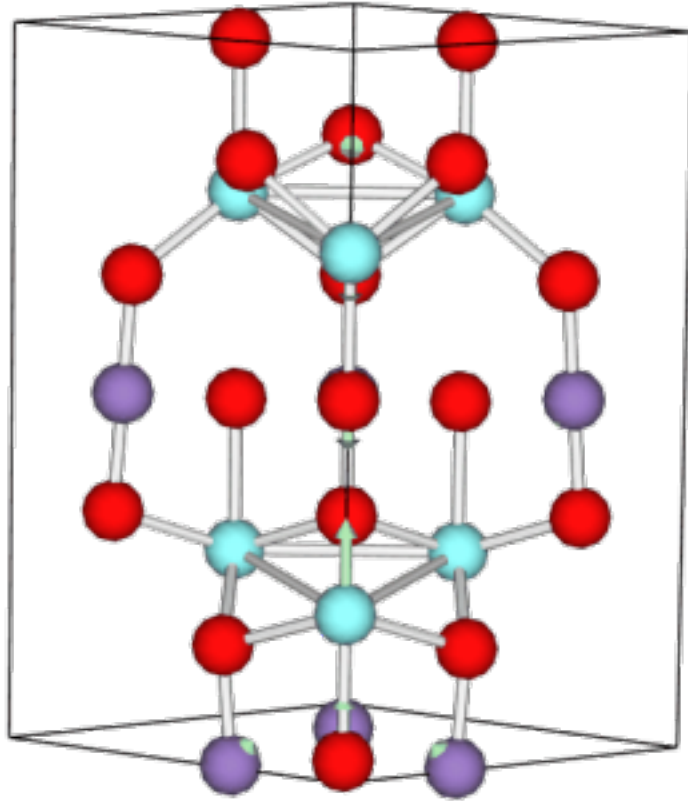
$$= \begin{pmatrix} E_{mag}(\mathbf{k}) & g_{\mathbf{k},\lambda}^{\dagger} & 0 & g_{\mathbf{k},\lambda} \\ g_{\mathbf{k},\lambda} & E_{ph}(\mathbf{k},\lambda) & g_{\mathbf{k},\lambda}^{\dagger} & 0 \\ 0 & g_{\mathbf{k},\lambda} & E_{mag}(\mathbf{k}) & g_{\mathbf{k},\lambda}^{\dagger} \\ g_{\mathbf{k},\lambda}^{\dagger} & 0 & g_{\mathbf{k},\lambda} & E_{ph}(\mathbf{k},\lambda) \end{pmatrix}$$

Mode-dependent  
magnon-phonon coupling strength



K point ( $1/3 \ 1/3 \ 0$ ), 8<sup>th</sup> phonon mode (16.17 meV)

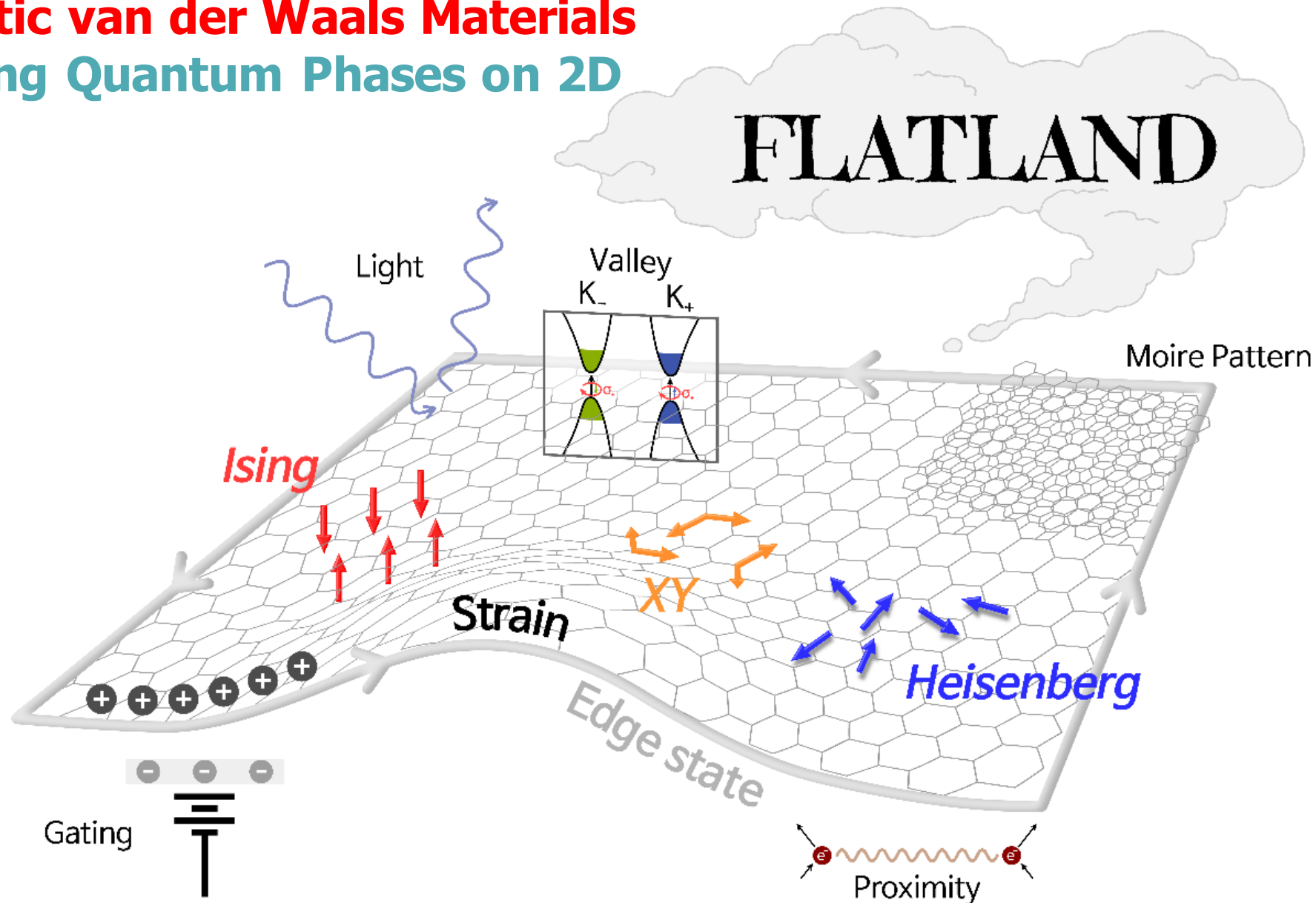
→ Mn-trimer breathing phonon mode is most strongly coupled with the magnons at K point.



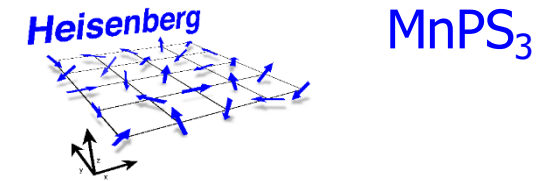
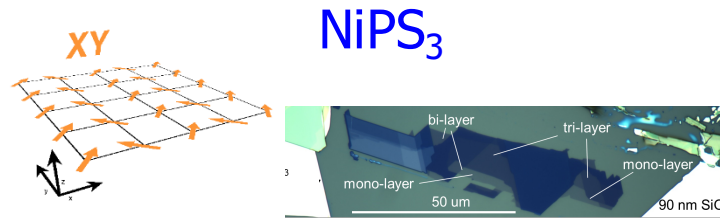
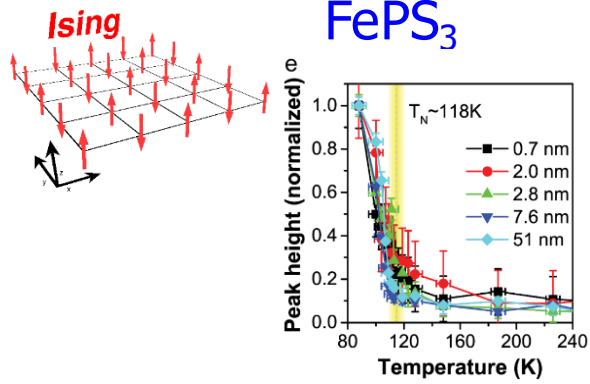


# 2D magnetic van der Waals Materials

## Landscaping Quantum Phases on 2D



Je-Geun Park, J. Phys. Condens. Matter 28, 301001 (2016)  
K. S. Burch, D. Mandrus & Je-Geun Park, Nature 563, 47 (2018)



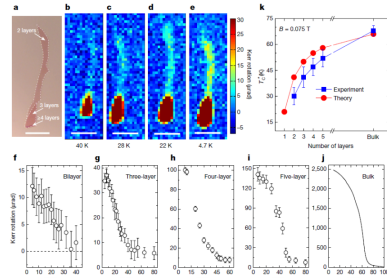
Jae-Ung Lee, JGP, Hyeonsik Cheong et al., Nano Lett. 16, 7433 (2016)

- S. Kim, JGP et al., Phys. Rev. Lett. 120, 136402 (2018)
- Kangwon Kim, JGP, Hyeonsik Cheong et al., Nat. Comm. 10, 345 (2019)
- Carina Belvin, JGP, Nuh Gedik, (in preparation)

- K. Kim, JGP, Hyeonsik Cheong et al., 2D Materials (2019)
- H. Chu, JGP, D. Hsieh et al., PRL (submitted)

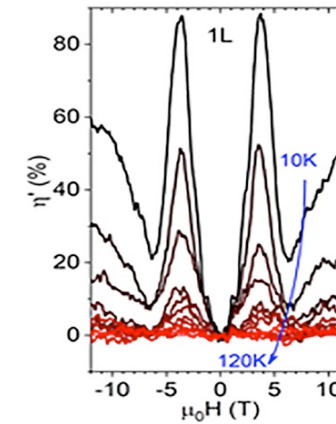
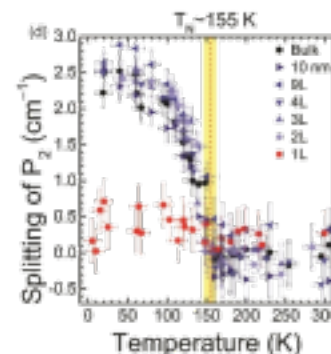
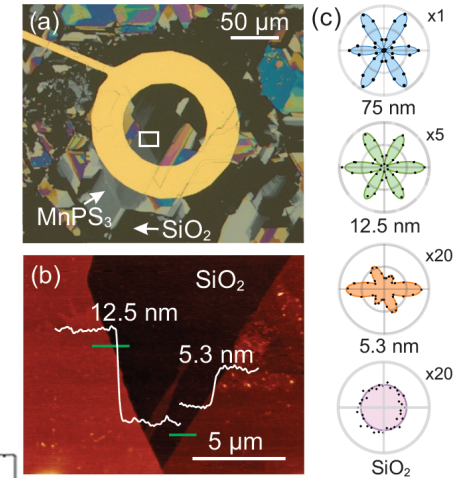
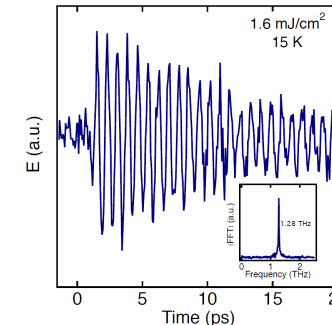
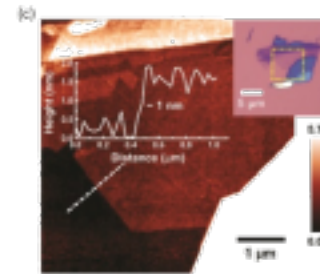
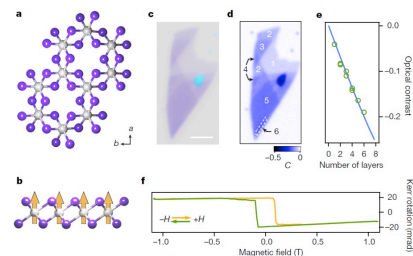
**CrGeTe<sub>3</sub>**

C Gong et al., Nature, 546, 265 (2017)



**CrI<sub>3</sub>**

B. Huang et al., Nature, 54 270 (2017)



\* Interesting Tunneling data from A. Morpurgo (submitted)

## Honeycomb Lattice

- Most of magnetic van der Waals materials have honeycomb lattice
- Ising:  $\text{FePS}_3$ ,  $\text{CrI}_3$ ,  $\text{VI}_3$ ,  $\text{Fe}_3\text{Ge}_2\text{Te}_6$  ...
- XY:  $\text{NiPS}_3$
- Heisenberg:  $\text{MnPS}_3$

cf:  $\text{RuCl}_3$

## Triangular Lattice

- 1T –  $\text{TaS}_2$ : possible quantum spin liquid state
  - M. Kratochvilova, NPG Quantum Materials 2, 42 (2017)
  - Y. J. Yu, Phys. Rev. B 96, 081111(R) (2017)

cf: Y Matsuda's talk on Tuesday

## Kagome Lattice

- $\text{Pd}_3\text{P}_2\text{S}_8$
- $\text{Nb}_3\text{I}_8$
- $\text{Nb}_3(\text{Br}, \text{Cl})_8$



# Acknowledgements

- Key Players at my group

**Kisoo Park, Joosung Oh**, Ki Hoon Lee, Manh Duc Le, Jaehong Jeong,  
J. C. Leiner, Je-Geun Park (CCES, SNU)



- Sample preparations

Hasung Sim (CCES, SNU)  
Hiroshi Eisaki & Yoshiyuki Yoshida (AIST, Japan)  
S. W. Cheong (Rutgers, USA)



- Neutron & x-ray experiments

T. G. Perring & Hyungje Woo (ISIS, UK)  
Kenji Nakajima & Seiko Ohira-Kawamura (J-PARC, Japan)  
Zahra Yamani, W. J. L. Buyers (AECL, Canada)  
A. Q. R. Baron (Spring8, Japan)



- Theoretical supports

Ho-Hyun Nahm, Ki Hoon Lee (CCES, SNU)  
A. L. Chernyshev (UCI, USA)



Jaehong Joeng

Taehun Kim

Kisoo Park



Kihoon Lee

Joosung Oh



- We have several positions open at the moment. If interested, please contact us.

- Strong magnon-phonon coupling produces a new hybrid magneto-elastic mode.
- We developed a quantitative formalism/procedure how to combine magnon and phonon.
- We provide a detailed momentum- and mode- analysis on the effect of magnon-phonon coupling.
- More general remark: In a noncollinear magnet, magnon mixes with other magnon and phonon, resulting in a creation of magneto-elastic excitation.

